2018

Geophysical Exploration of the Upper Crust Underlying North-Central Indiana: New Insight into the Eastern Granite-Rhyolite Province

Michael Ray Green
Wright State University

GEOPHYSICAL EXPLORATION OF THE UPPER CRUST UNDERLYING NORTH-CENTRAL INDIANA: NEW INSIGHT INTO THE EASTERN GRANITE-RHYOLITE PROVINCE

A thesis submitted in partial fulfillment of the requirements for the degree of

Masters of Science

By

MICHAEL RAY GREEN II

B.S. Concord University, 2015

2018

Wright State University

WRIGHT STATE UNIVERSITY

GRADUATE SCHOOL

April 19, 2018

I HEREBY RECOMMEND THAT THE THESIS PREPARED UNDER MY SUPERVISION BY Michael Ray Green ENTITLED Geophysical Exploration of the Upper Crust Underlying North-Central Indiana: New Insight into the Eastern Granite-Rhyolite Province BE ACCEPTED IN PARTIAL FULFILLMENT OF THE REQUIREMENTS FOR THE DEGREE OF Master of Science.

Ernest Hauser, Ph.D.
Thesis Director

David F. Dominic, Ph.D.
Chair, Department of Earth &
Environmental Sciences

Committee on
Final Examination

Ernest C. Hauser, Ph.D.

Doyle R. Watts, Ph.D.

David F. Dominic, Ph.D.

Barry Milligan, Ph.D.
Interim Dean of the Graduate School

ABSTRACT

Green II, Michael Ray, M.S., Department of Earth and Environmental Sciences, Wright State University, 2018. Geophysical Exploration of the Upper Crust Underlying North-Central Indiana: New Insight into the Eastern Granite-Rhyolite Province

This study analyzes ten 2D seismic lines donated by CountryMark together with potential field data to examine the upper crustal structure near Wabash, Indiana. These seismic profiles reveal significant relief of the Precambrian Unconformity and prominent upper crustal reflections. The Precambrian Unconformity interpreted from the unmigrated stacked seismic sections is characterized by undulations and bowtie artifacts. Zero offset seismic models constructed using profiles of the exposed Precambrian Unconformity across the Eastern Granite-Rhyolite Province outcrops of the St. Francois Mountains feature the same seismic expression. The upper crust below the Precambrian Unconformity on the Countrymark seismic sections is also characterized by discontinuous high-amplitude reflections that occur ~0.5s two-way time below the Precambrian Unconformity. The distribution of these upper crustal reflections on a time structure map correlates with positive magnetic and gravity anomalies suggesting the reflectors are likely mafic. These geophysical observations are consistent with a scenario like that interpreted for the evolution of the Precambrian rocks of the St. Francois Mountains and also the findings of McBride et al. (2016) for patterns of reflections on seismic lines in central Illinois.

TABLE OF CONTENTS

Page

LIST OF FIGURES

Page

List of Acronyms

CDP-Common Depth Point

CM-CountryMark

CMP-Common Midpoint

CPO-Central Plains Orogeny

EGRP-Eastern Granite Rhyolite Province

FWA-Fort Wayne Anomaly

GO-Grenville Orogeny

GP-Grenville Provence

IGWS-Indiana Geological & Water Survey

MCR-Midcontinent Rift

MGSC-Midwest Geological Sequestration Consortium

MHA-Miami Howard Anomaly

MKA-Marshall Kosciusko Anomaly

NAMC-North American Midcontinent

PO-Penokean Orogeny

RFA-Rush Franklin Anomaly

SGRP/WGRP-Southern Granite Rhyolite Province/also known as Western Granite Rhyolite Province

THO-Trans Hudson Orogeny

WMA-Wabash Miami Anomaly

1.0 Introduction

1.1 Relevance

The Eastern Granite-Rhyolite Province (EGRP) is a Mesoproterozoic province of the North American Midcontinent basement region (Fig.1). The EGRP overlaps and overprints the older Central Plains Orogenic Province (CPO) to the west and is physically bound by the younger Grenville Province (GP) to the East. The EGRP is separated from the Southern/Western Granite-Rhyolite Province (SGRP/WGRP) to the south by a transitional change in the age of granitic magmatism of the two provinces. The St. Francois Mountains of SE Missouri are the only outcrops of rocks of the EGRP. The remaining portion of the EGRP is masked by thick Paleozoic sedimentary sequences. Our current understanding of the composition and formational history of the EGRP apart from the St Francois Mountain exposures is limited core samples from dispersed deep boreholes, scattered seismic reflection surveys, an incomplete potential field database that is largely half a century old.

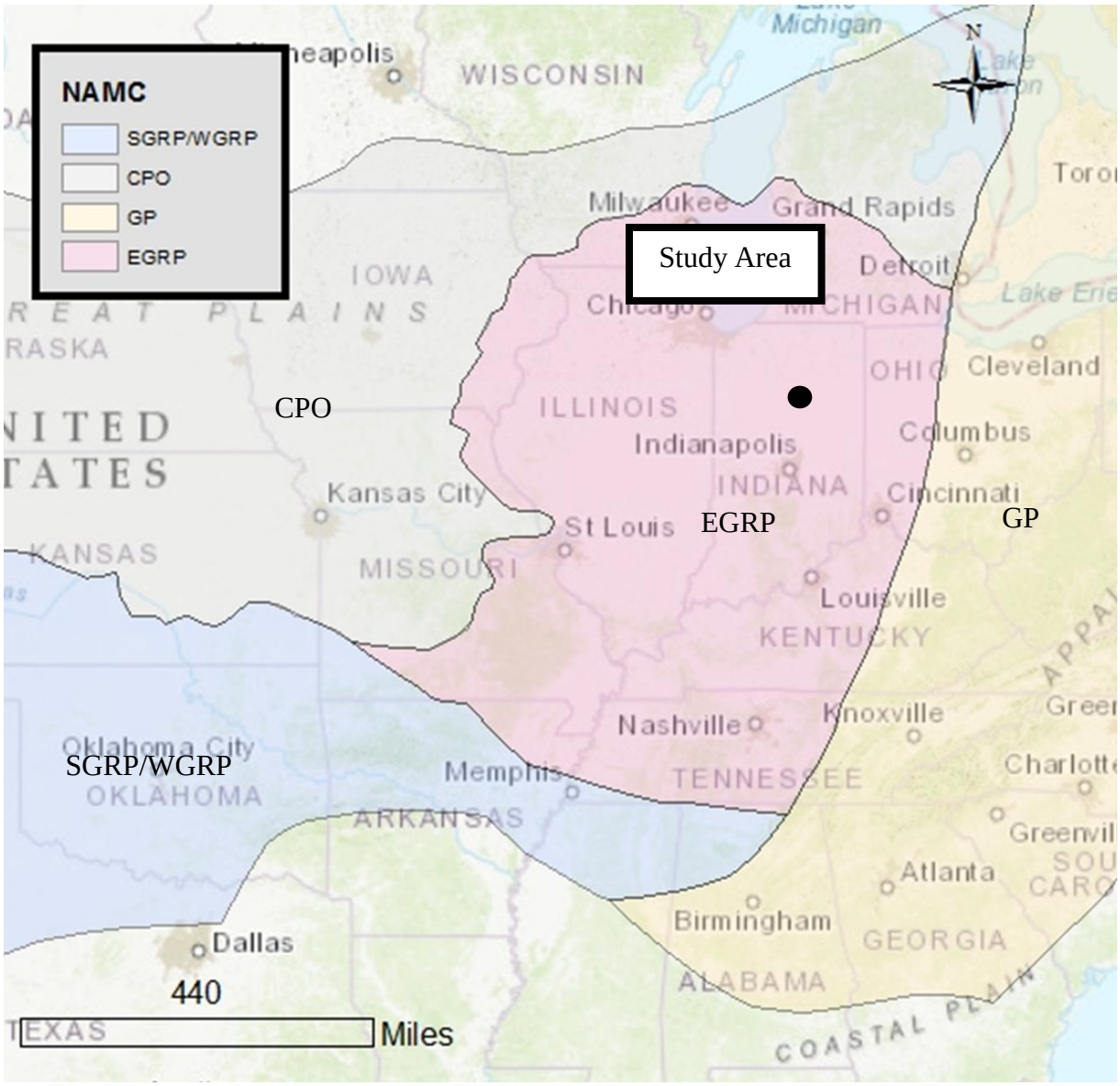

Figure 1: Generalized map of the Eastern Granite-Rhyolite Province and surrounding basement provinces. (Modified from Bickford et al., 2015).

1.2 Objectives

This study is fundamentally stimulated by the availability from CountryMark of ten 2-D seismic reflection lines located in north-central Indiana near the city of Wabash (Fig.2). This study seeks to characterize the geology associated with the two main features evident on these seismic lines. One feature of these data appears as the Precambrian unconformity characterized by distinctive bow-tie structures and diffractions in the unmigrated seismic data at the base of the layered Paleozoic sequence. This interpretation is examined in this study through comparison with zero-offset ray-trace modeling of the exposed relief of the Precambrian unconformity in the St. Francois Mountains of southeast Missouri. The second prominent feature of these data consists of a high amplitude zone of reflections and apparent diffractions that occur within the underlying Precambrian crystalline basement. Analysis of these deeper reflections are examined in this study also through zero-offset ray-trace modeling to develop a plausible geological interpretation, but also examined in relation to potential field data. Existing aeromagnetic data are available for the study area and appear sufficient for analysis; but, due to the extreme sparseness of existing publicly available gravity data an extensive new gravity dataset has been collected as a part of this study.

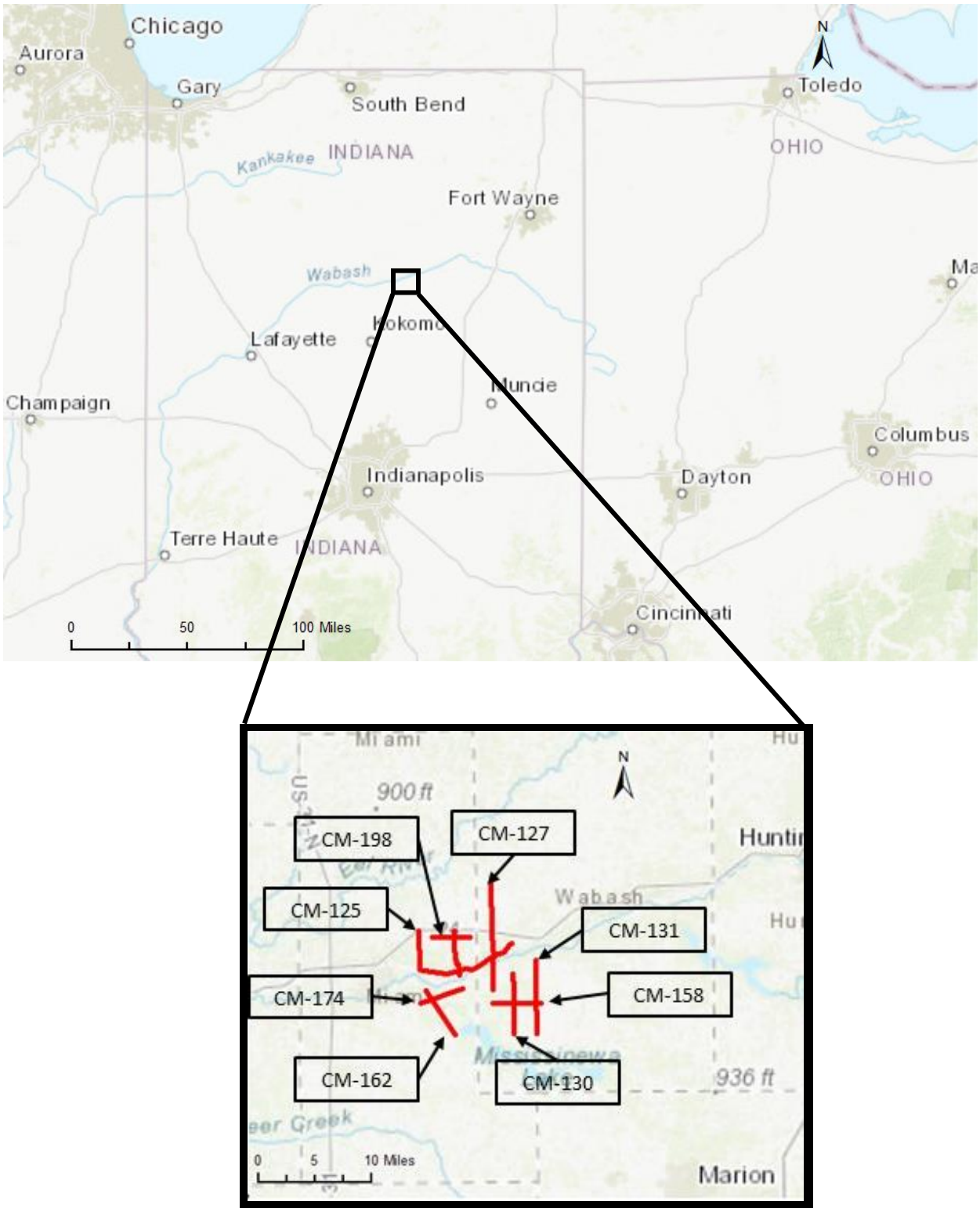

Figure 2: Geographic location and orientation of the ten newly available seismic lines collected by CounrtyMark. The location of the seismic lines is centered on Wabash and Peru, Indiana.

2.0 Background

2.1 The North American Midcontinent

2.1.1 General Description

In the context of the Precambrian continental assemblage of southern Laurentia, the North American Midcontinent (NAMC) is generally defined as the geologic region bound by the Rocky Mountains in the West and the Appalachian Mountains in the east (Bickford et al., 2015). The crystalline Precambrian basement of the NAMC region has been separated into provinces comprising various metamorphic and igneous lithologies characterized by processes of long-lived convergent tectonics combined with less frequent periods of extensional tectonism that occurred throughout Proterozoic time (Bickford et al., 2015). The end of continental growth is marked by the end of Grenville related compression ~0.7 Ga and the subsequent deconstruction of the supercontinent Rodinia (Evans, 2009).

2.1.2 Precambrian Assemblage

The southern NAMC provinces began to assemble when the Archean Superior and Wyoming provinces were welded together by the Trans-Hudson Orogeny (THO, ~2.0 Ga), which was closely followed by events of the Penokean Orogeny (PO, ~1.88 Ga). Subsequent (post ~1.8 Ga) juvenile volcanic terrains were accreted to the southern margin of the growing continent and collectively termed the Central Plains Orogen

(CPO) which continued with convergence and accretion for another 0.2 billion years. The CPO was then quickly followed by the development of the Granite-Rhyolite Provinces which occurred between ~1.55 and 1.27 Ga. The history of convergence and accretion was briefly interrupted ~1.25 Ga by development of the Midcontinent Rift, but the Precambrian assemblage of the NAMC was concluded with the compressional events of the Grenville Orogen (GO, ~1.1 to 0.9 Ga).

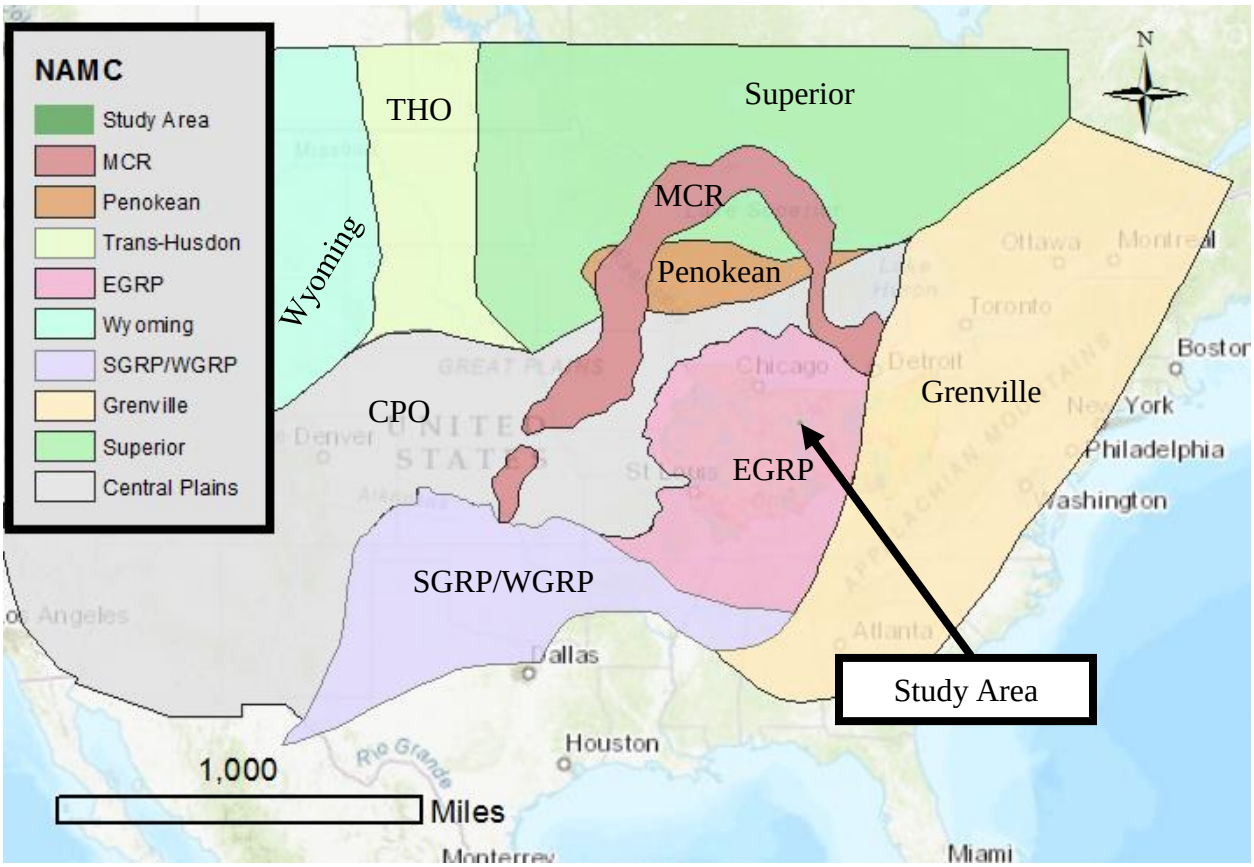

Figure 3: Summary of southern NAMC basement provinces which includes generalized boundaries (Modified from Bickford et al., 2015).

2.2 The Granite-Rhyolite Provinces

2.2.1 The Evolution of Ideas

The tectonic setting that led to the emplacement of the enigmatic felsic igneous plutons that are thought to make up the bulk composition of the Granite-Rhyolite Provinces has been a topic of academic debate for decades. Studies published during the early 1980's established what can be considered two different academic camps championed by slightly contrasting theories. The first of the two camps drew upon the classical association of A-type plutonism's and crustal anataxis (Anderson and Cullers, 1978; Emslie, 1978; Anderson, 1983). This camp generally favored a simplistic model involving a failed rift and used the east African rift as a modern analogue (Anderson, 1983). The second group favored derivation from a long-lived convergent boundary and placed emphasis on the lack of kinematic evidence supporting emplacement via a purely extensional tectonic regime (Van Schmus and Bickford, 1981).

In the late 1980's additional isotopic data helped start to refine the theories involving the evolution of the granite-rhyolite province. Also, a general consensus developed by the further discovery of more widely dispersed mafic intrusive bodies thought to have been in support of A-type derivation of silicic magmas via extensional tectonism. Additionally, a lack of evidence supporting the crustal thickening required by the earlier model published by Bickford and Van Schmus (1981) was also a factor in the development of this consensus (Bickford and Van Schmus, 1986). An early samarium-

neodymium (Sm-Nd) geochronological study of cores from the Granite-Rhyolite Provinces suggested that parent materials couldn't have been older than 1800±100Ma indicating that at least a portion of the Granite-Rhyolite Provinces were likely derived from crust accreted onto the eastern portion Laurentia during Paleoproterozoic events of the Central Plains Origin. As a result, Bickford and Van Schmus (1986) suggested that the rocks of the Granite-Rhyolite Provinces were likely a thin veneer of a few kilometers thick that intrude and overlie the older crust of the CPO region.

Soon after the theory for the anatectic melting of Paleoproterozoic rocks, probably as a result of rifting, became widely accepted, reports from Sm-Nd analysis of samples from the EGRP further complicated the history of the region. New Sm-Nd data first reported during the early 1990's showed that the igneous rocks of the EGRP were not only derived from the rocks of the earlier Paleoproterozoic CPO event, but that at least a portion of the Granite-Rhyolite Provinces (SE of the Sm/Nd line on Fig. 4) was derived from younger Mesoproterozoic crustal sources (Van Schmus et al., 1993).

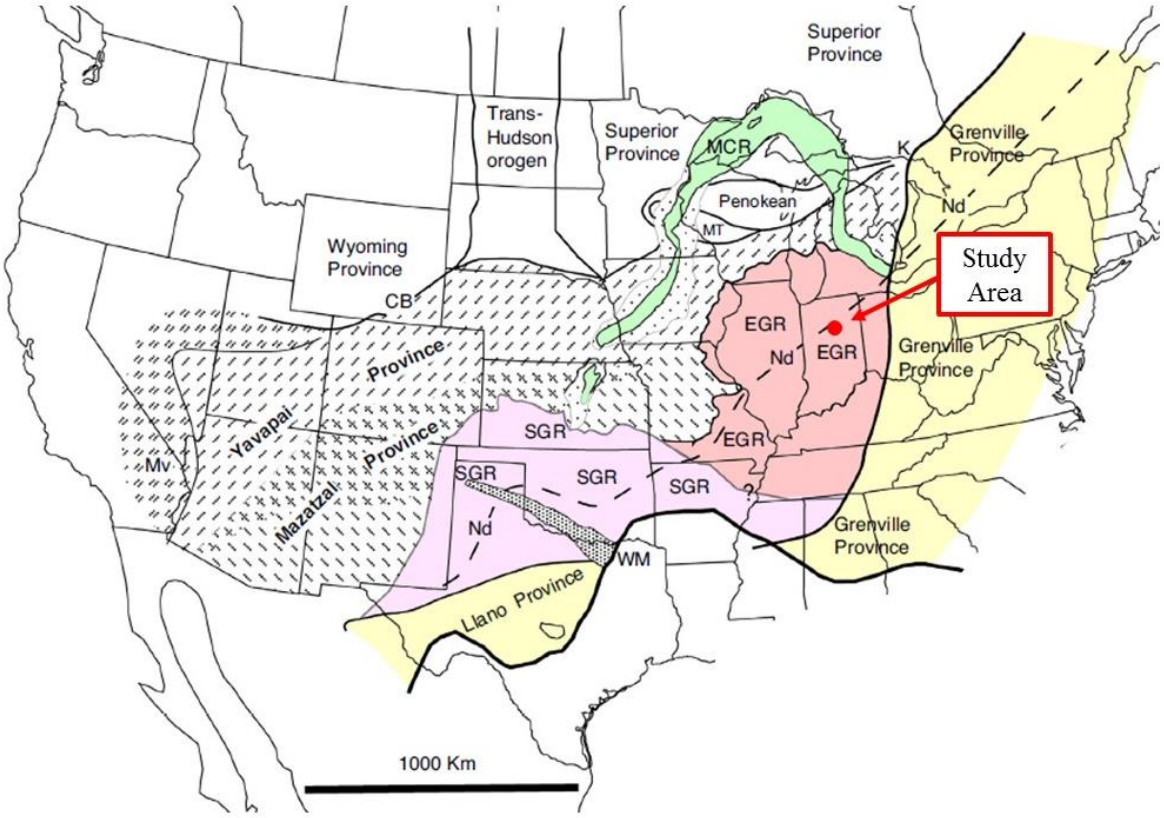

Figure 4: Bickford et al.'s figure of the southern NAMC basement provinces. The Sm-Nd (dashed) line splits the Granite-Rhyolite provinces into West and East sections. The west section represents rocks of the two Mesoproterozoic provinces likely derived from Paleoproterozoic crustal sources while the east section represents rocks derived from Mesoproterozoic sources (Bickford et al. 2015).

2.2.2 Current Model

A recently published paper (Bickford et al., 2015) proposes a theory of Granite-Rhyolite Province evolution that is generally consistent with all significant geological and geophysical observations made of the two provinces to date. This model begins ~1.5 Ga with the development of an active tectonic margin across the present southeastern margin of Laurentia. Convergence and subduction of oceanic crust was accompanied by the formation of a volcanic arc on the margin of the continent as well as the formation of juvenile outboard arcs (Bickford et al., 2015). Convergence along the margin is also thought to have led to crustal weakening and possible delamination and underplating of basaltic magma that resulted in interior cratonic back-arc spreading and the likely mechanism that gave rise to the felsic magmatism west of the Sm-Nd line that defines the margin of older accreted crust (Bickford et al., 2015). Juvenile outboard arcs are thought to have been rapidly accreted to the margin around the same time, and a similar succession of events is presumed to have given rise to the younger granitic rocks observed in the NE portion of the EGRP.

2.2.3 The St. Francois Mountains

The St. Francois Mountains of SE Missouri (Fig. 5) are the only outcrops of the EGRP and is tentatively categorized into a volcanic suite and a sub-volcanic intrusive suite. The volcanic suite dominates the western outcrops and consists predominately of felsic ash flow tuff (Sides et al., 1981). The plutonic suite dominates the eastern outcrops

and is mainly composed of crystalline felsic lithologies with a substantially smaller component of mafic material (Kisvarsanyi, 1980). Large portions of the St. Francois Mountains are occupied by granite ring structures and Dr. Kisvarsanyi developed a popular theory describing the evolution of these complexes wherein they developed during three main periods (Fig. 6) (Kisvarsanyi, 1980):

I. Regional uplift as a product of the emplacement of subvolcanic felsic massifs and comagmatic volcanism followed by cauldron depletion and associated subsidence creating fracture networks around the outer edge of the complex.

II. Emplacement of ring dykes along outer fracture network. Dykes have been reported as mostly being composed of amphibole granites with a smaller likely component of basic material.

III. Resurgent doming as a result of a central pluton rising into the subsided cauldera.

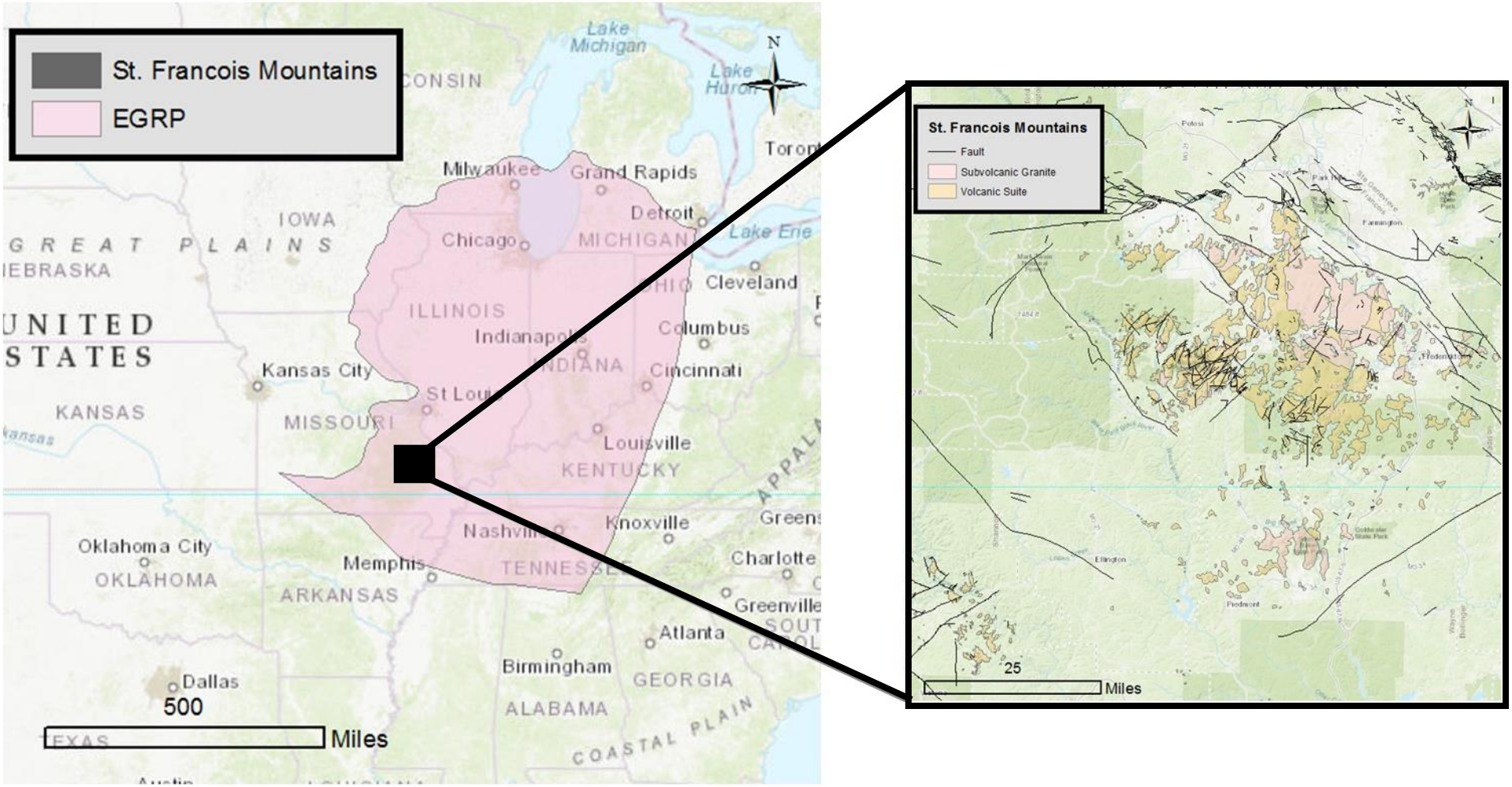

Figure 5: Location of the St. Francois Mountains with respect to the entire EGRP. The St. Francois Mounatins fall to the south of Bickford et al.'s Nd-Sm model line meaning that the igneous rocks belonging to the St. Francois Mountains and surrounding area are derived from juvenile crustal sources. U-Pb data places the formation of the various intrusive rocks belonging to SFM at between ~1.5-1.35Ga (Bickford et al., 2015).

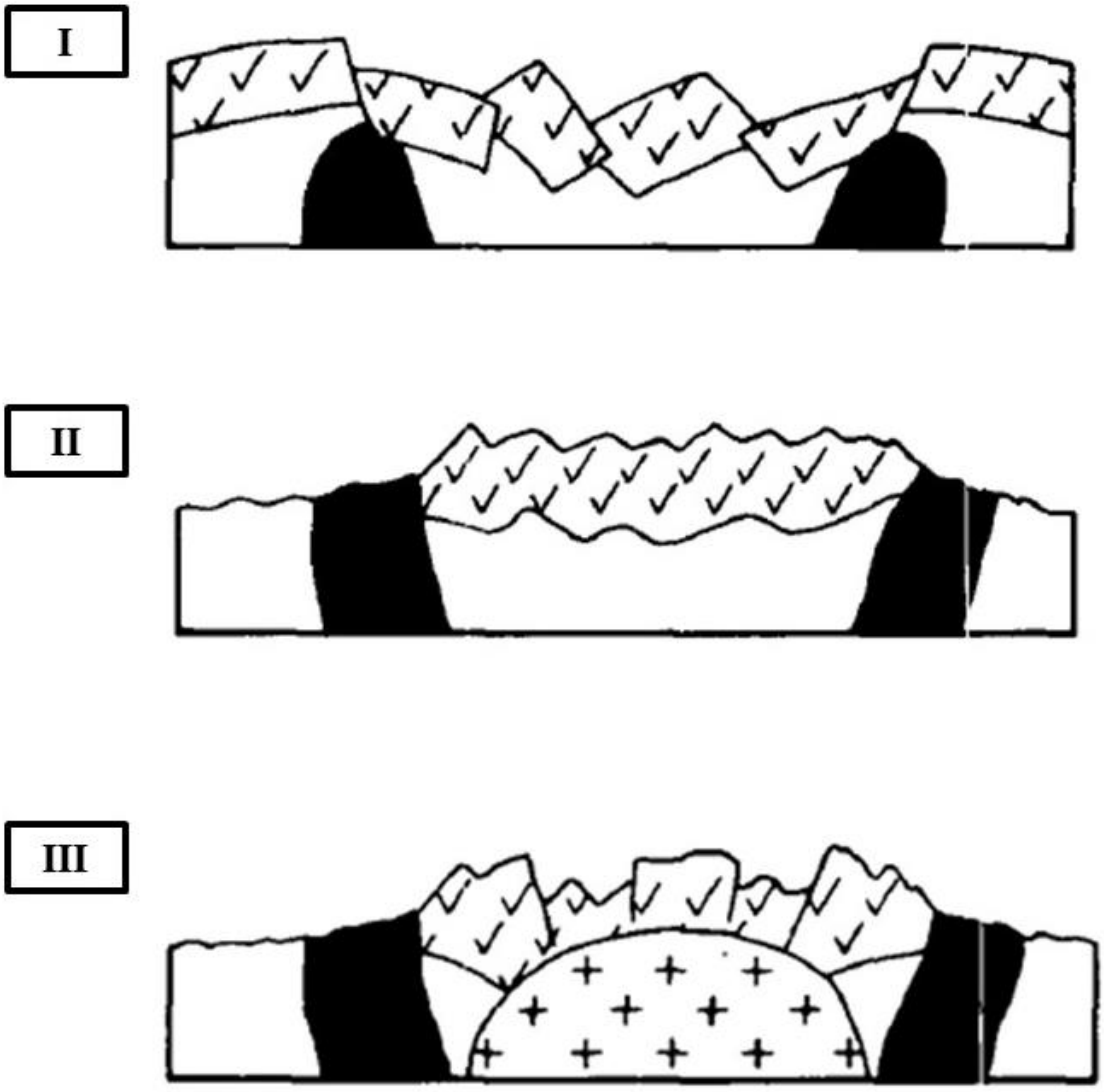

Figure 6: The model of Dr. Kisvarsanyi describing the evolution of granitic ring complexes in the St. Francois Mountains. (Modified from Kisvarsanyi, 1980).

2.3 Similar Geophysical Studies of the EGRP

2.3.1 Seismic Reflection Studies

Only a handful of modern seismic reflection studies have imaged the Precambrian crystalline rock associated with the Eastern Granite Rhyolite Province. The earliest of these studies were carried out by the Consortium for Continental Reflection Profiling (COCORP) funded by the National Science Foundation (NSF). The COCORP project gathered deep seismic reflection data across central Ohio, southern Indiana, southern Illinois and into Missouri in the 1980's. Publications of interpretations involving the COCORP seismic reflection line OH 1 (Fig.7) identified the Grenville Front Tectonic Zone and intra-Grenville crustal structures (Culotta et al., 1990) and also indicated that a foreland thrust belt and a possible Grenville foreland basin may lie west of the Grenville Front (Hauser, 1993). Layered rocks were also detected within the Precambrian crust on the the Indiana and Illinois COCORP lines which were interpreted to likely be composed of layered volcanic or sedimentary rocks and termed the Centralia Sequence (Pratt et al., 1992).

One of the most recent seismic reflection data sets imaging the EGRP was carried out by the Midwest Geological Sequestration Consortium (MGSC) with the goal of characterizing the Paleozoic sedimentary units of the Illinois Basin and the underlying crystalline Precambrian crust for purposes of CO_2 sequestration. The MGSC project, termed the Illinois Basin Decatur Project (IBDP), gathered 124 miles of high resolution

2D seismic reflection data in the form of three 2-D lines that meet and cross in central Macon County (Fig.7) where the MGSC also gathered a large high-resolution 3D data set (McBride et al., 2016; Smith and Leetaru, 2014). McBride and others (2016), published interpretations of the Precambrian interval observed on the four seismic data sets that included high relief paleotopography at the base of the Mount Simon Sandstone and two types of high amplitude seismic features found within the felsic igneous rocks of the EGRP. The first and largest of the two seismic features appears to coincide well with a positive aeromagnetic anomaly and is interpreted to be a large bowl shaped mafic intrusive system interpreted to represent a large sill and dike system (McBride et al., 2016). The second and more isolated of the seismic features is typically observed in various locations below the high amplitude reflections of the larger interpreted mafic intrusive system and have been interpreted as isolated sills or small stocks.

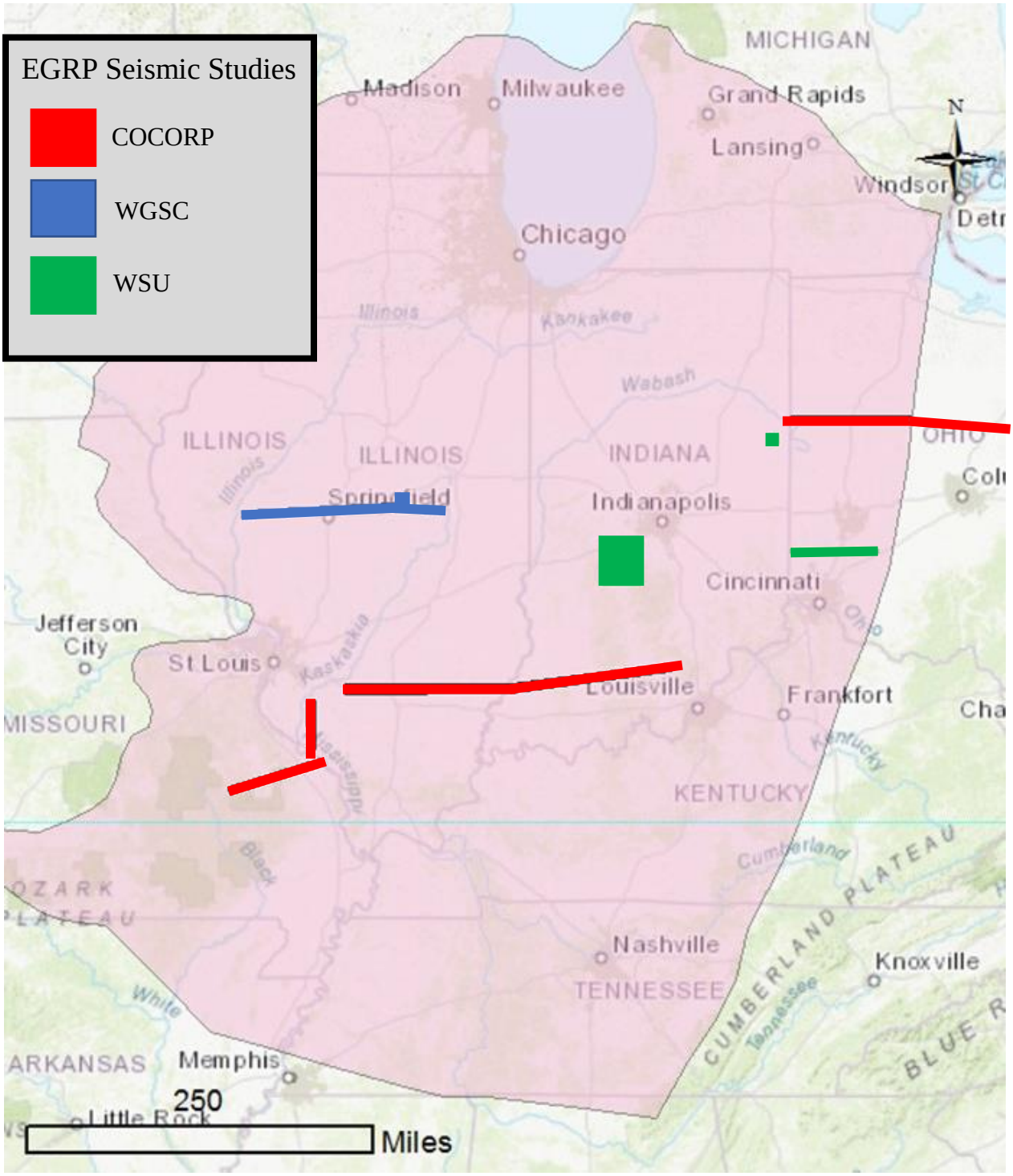

Figure 7: General locations of seismic work discussed in this study. Most other seismic studies have been carried out in Kentucky. One example would be the two seismic lines gathered by the Kentucky Geological Survey located in Western Kentucky (Drahovzal, 1997).

2.3.2 Potential Field Studies

Aeromagnetic and gravity methods have been employed in both large scale, like defining the boundaries of different NAMC provinces, and small scale studies of isolated distinct anomalies. The pattern dominating the EGRP has been described as generally subdued with numerous circular gravity and magnetic anomalies (Atekwana, 1996). It has been proposed that this pattern is likely a function of the granitic country rock being intruded by dispersed mafic plutons associated with rifting (Bickford and Van Schmus, 1986; Atekwana, 1996). Rudman et al. (1971) describe one such circular potential field anomaly in Hamilton County, Indiana, as being best represented by a vertical pipe associated with overlying flows of diabase material. Rudman and Blakely (1965) also examined the circular dipole anomaly observable in Pulaski County, Indiana, which they interpreted to be a mafic plug. These studies employed early modeling methods that calculated potential fields from basic 2D geometric models (Rudman and Blakely, 1965; Rudman et al., 1971). Other textbook cases of such anomalies have been noted elsewhere within Indiana in Elkhart and Grant Counties (Henderson and Zietz, 1958). McBride et al. (2016) made use of vertical derivative potential field maps, most notably aeromagnetic, in an attempt to define the edges of such regional scale anomalies to the zero contour to match reflection-defined bodies found in seismic reflection surveys (McBride et al., 2016). Specifically, they used first vertical derivative maps of the reduced-to-pole magnetic field to support their interpretation of a large bowl-shaped set of reflectors that they interpreted to likely be a sill complex composed of mafic igneous rock.

2.4 Post Precambrian Geology

2.4.1 Regional Paleozoic Stratigraphy

The ten seismic lines of this study provided by CoutnryMark are located on the NE side of the Illinois Basin in the vicinity of the Kankakee Arch (Fig. 8A). This study does not explore the details of the Paleozoic stratigraphy evident on the seismic data. Consequently, only a general summary of the major Paleozoic stratigraphic units present is warranted. The main stratigraphic units include the Mount Simon Sandstone, Eau Claire Formation, Knox Supergroup, Ancell Group, Black River Group and the Trenton Limestone. Figure 8A is an excerpt from the general stratigraphic column developed by the Indiana State Geological Survey (Shaver et al., 1986) showing the relationship of these stratigraphic units.

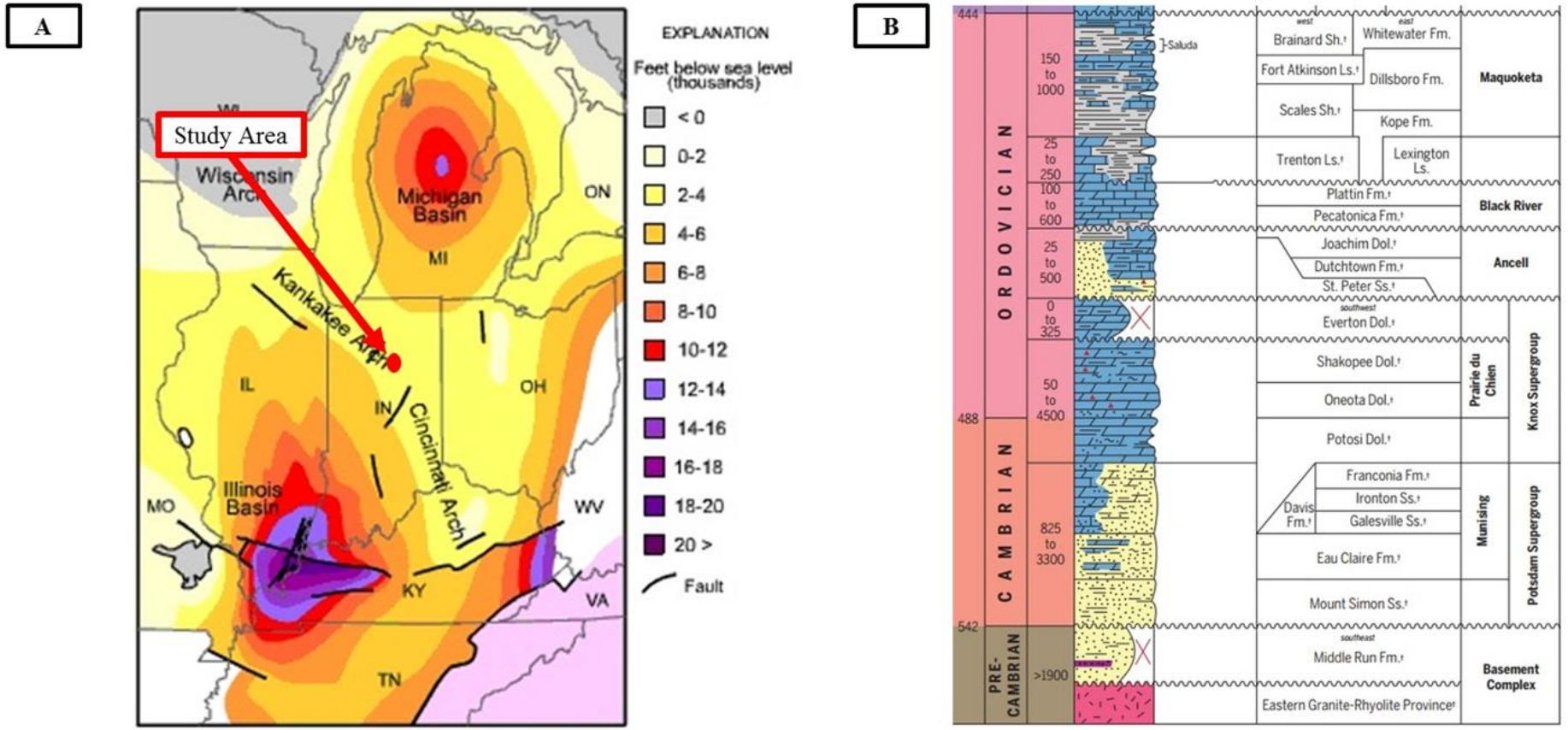

Figure 8: (A) Paleozoic sedimentary provinces overlying the SE portion of the NAMC (Modified from Droste and Shaver, 1983; Rudman and Rupp 1993). **(B)** Excerpt from the generalized stratigraphic column of Indiana (Shaver et al., 1986). Several of the stratigraphic units described in this excerpt are not apparent on the seismic sections or may even possibly be absent in the subsurface. These units include the Black River Group, the Ancell Group and the Middle Run Formation.

2.4.2 Near Surface Sediment Deposits

The depth to bedrock in the vicinity of the study varies from ~10' to 200'+ (~3m to 70+m). This variation is a product of the various fluvial and glacial events following the deposition and lithification of the underlying Paleozoic bedrock. The complex history of glacial and fluvial events left behind a variety of different unconsolidated sedimentary deposits that make up the seven currently identified aquifer systems of Wabash and Miami counties (Grove, 2007; Unterreiner, 2007). Figure 9 is a modified version of the maps developed by the Indiana DNR and are almost exclusively based on water well logs.

Bedrock depth observations in Wabash and Miami counties define a pre-glacial drainage system that cuts east to west across the counties (Fig. 9). The system is described as a deeply buried bedrock valley filled primarily with sand and gravel deposits (Grove, 2007; Unterreiner, 2007), and has been interpreted to be associated with the ancient Teays River (Hansen, 1995). The Teays river once drained much of the central Appalachian Mountains and coursed across Ohio, Indiana and Illinois prior to being rerouted by the Pleistocene glaciation that occurred ~2 million years ago (Hansen, 1995). These glacial advances buried the Teays in the western part of Ohio and across Indiana and Illinois. The resulting avulsion is the modern Ohio River that now flows westward defining the southern boundaries of Ohio, Indiana and Illinois.

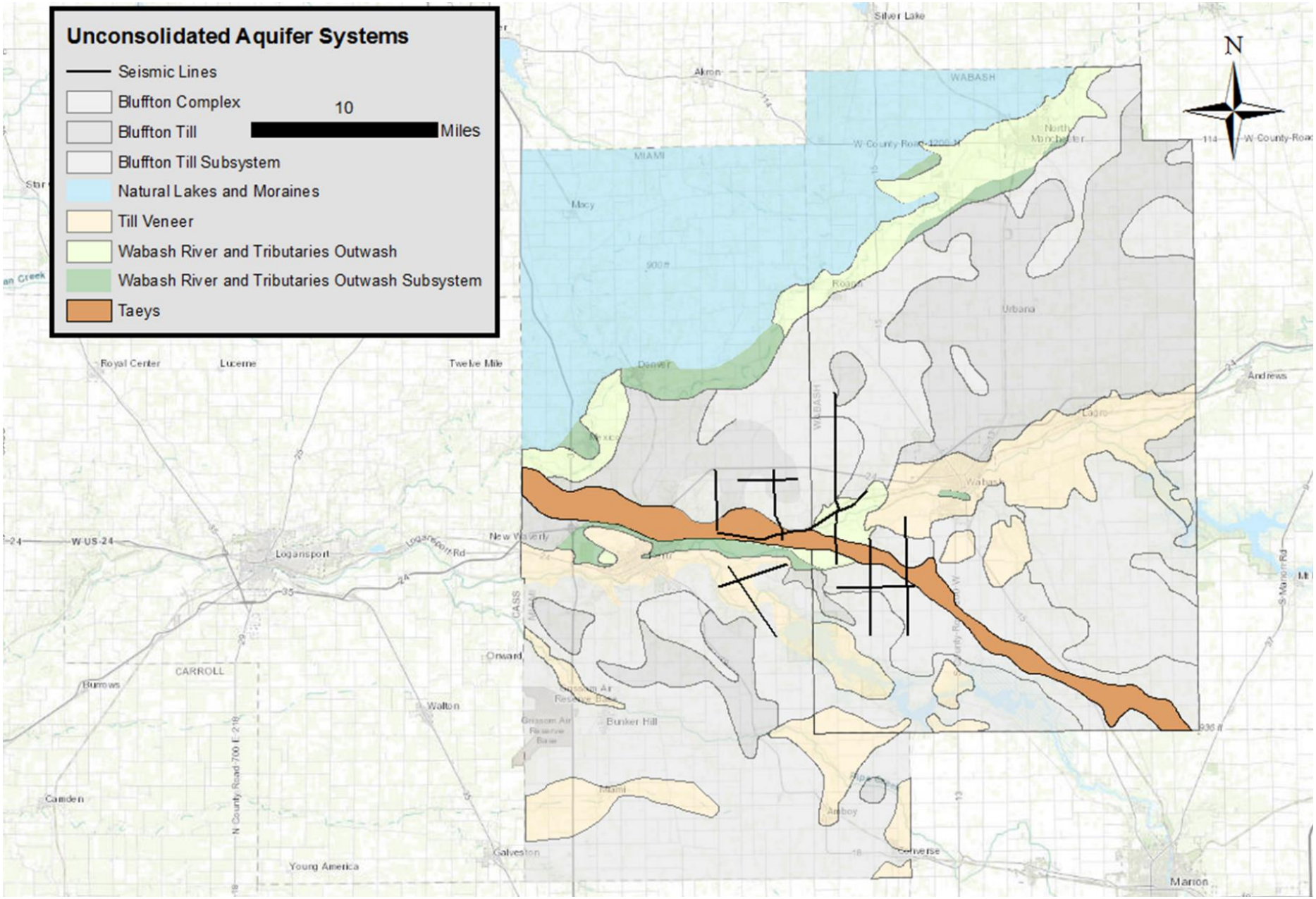

Figure 9: Modified maps of the unconsolidated aquifer systems of Wabash and Miami Counties Indiana published by the Indiana Department of Natural Resources (DNR). (Modified from Unterreiner, 2007 and Grove, 2007). The Teays system as a regional deep buried pre-glacial bedrock valley.

3.0 Methods

3.1 Seismic

3.1.1 Description of Dataset

The ten 2D seismic lines interpreted in this study were acquired by Bay Geophysical on behalf of CountryMark. Seismic data were gathered along public highways using a nominal station spacing of 55'. A vibroseis source was used in a roll-on/roll-off acquisition design. Vibroseis sources were operated at a peak force of 26,000lbs sweeping frequencies from 12 to 130Hz. The 8s sweeps included a 300ms ramp up and 100ms ramp down. The maximum number of live stations per shot gather was 163. With 10s of listening time, the 8s sweeps resulted in 2s of correlated data, sampled at a 1ms sample rate. The seismic data were processed by Geo Concepts Inc of Castle Rock, Colorado. Figure 10 is a flow chart that summarizes the processing flow of the stacked sections as reported in the seg-y headers by Geo Concepts Inc.

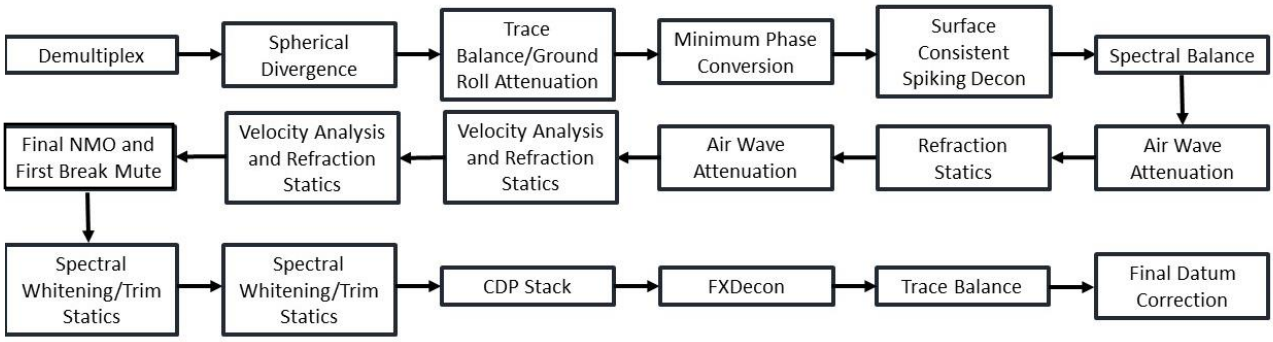

Figure 10: Processing workflow for all ten sections processed by Concepts Inc.

3.1.2 Visualization

Seismic and well log interpretation is primarily carried out using the 2016 version of IHS Kingdom Suite (TM, IHS). Kingdom Suite software utilizes several different modules that are all accessible via the primary user interface in order to effectively streamline and enhance the interpretation of geophysical data. VuPAK is the Kingdom 3D viewer and is used as quality control to evaluate picks where seismic lines cross in order to alleviate some of the possibility of picking structure that may be a product of sideswipe. SynPAK is the Kingdom synthetics package where synthetic seismic traces are formulated from wire line logs. GeoSyn2D is a standalone zero-offset ray-trace modeling program that can be launched from the primary module or separately, which is used in this study alongside SynPAK to evaluate picks made within the Paleozoic interval. GeoSyn2D uses a time-depth chart created in SynPAK and user-defined structural trends to create full scale models of seismic sections. Other software used in this study included Hampson-Russel, GSEGY-View, and Petrel (TM, Schlumberger).

3.1.3 Ray Trace Modeling

Ray trace modeling is commonly used in both the acquisition and interpretation of seismic reflection data. I employ ray tracing to study the Precambrian unconformity and other structures observed below the Precambrian unconformity on stacked unmigrated sections. For this purpose, zero-offset ray tracing is used to simulate pre-migrated stacked sections. Zero-offset ray tracing simulates stacked data by calculating ray paths assuming source and receiver pairs at the same location, therefore simulating data that has been

stacked from CMP gathers. Ray-trace modeling for this study is conducted using GXII two-dimensional geoscience modeling software developed and provided by ION Geophysical.

Ray trace modeling can be conducted as a forward, reverse or combination modeling practice. Forward ray-trace modeling involves building a two-dimension geologic depth section composed of layers with physical properties including lateral continuity, thickness and seismic wave velocity. These properties are then put through any of several different forms of ray tracing where source and receiver locations are input into the model. The final step transforms all of the inputs into the construction of trace data representing a seismic line. Reverse modeling, indicative of its terminology, works in very much the same way. It involves the importing of stacked seismic data, identification of reflections as the tops of layers and the input of seismic properties such as P-wave velocity. These inputs are then used to transform a time section directly into a depth section.

For this study, I employ both forward and reverse modeling in combination. The process begins as a reverse modeling exercise whereby a processed seismic time section is imported and transformed into a depth section. From this point the original Precambrian surface that reverse modeling derives is cut out and replaced with a topographic profile from a portion of the St. Francois Mountains dominated by EGRP granite (Fig. 11). Zero-offset ray tracing is then applied using source/receiver offsets identical to the CDP offset taken from the original stacked data that was imported from

the initial reverse modeling step. The modeling process is then completed by the plotting of traces and the adjustment of display variables such as noise and gain.

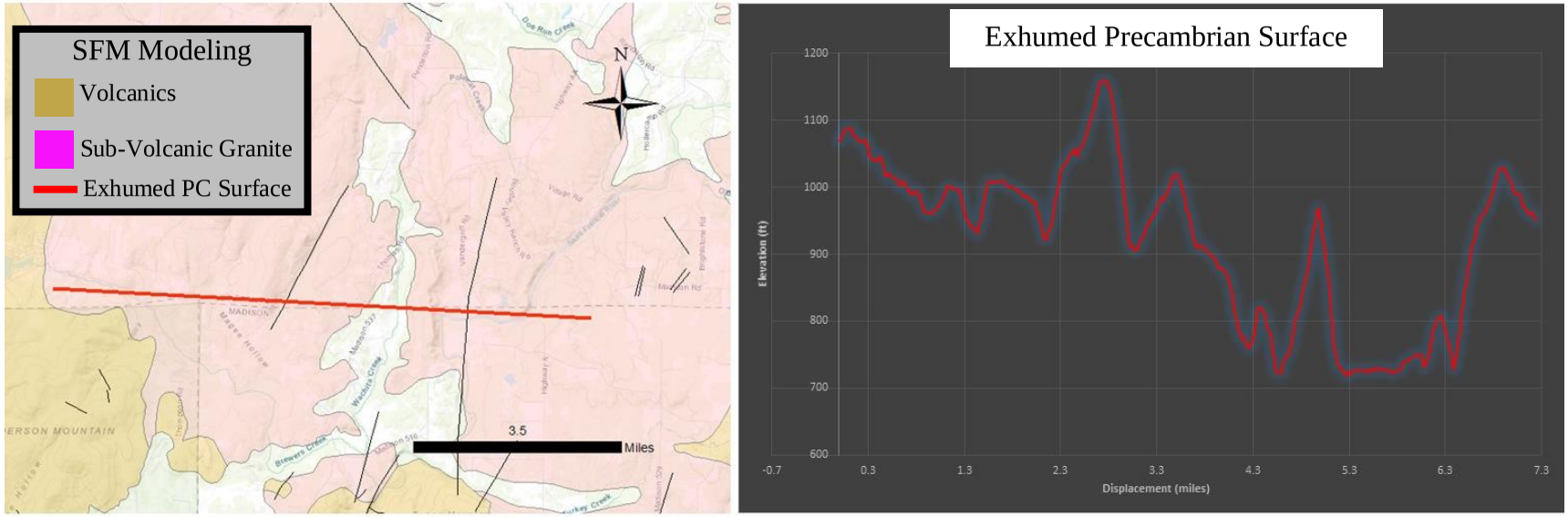

Figure 11: Topographic profile of the exhumed Precambrian surface extracted across the St. Francois Mountains sub-volcanic granite terrain used for zero offset ray trace modeling.

3.2 Applications of Well Logs

3.2.1 Synthetic Trace Formulation

A synthetic trace was constructed from well logs to relate the reflections of the seismic sections to Paleozoic stratigraphy (Fig. 12). Only the Paleozoic interval can be correlated using this method because there are no deep boreholes that sufficiently penetrate the Precambrian located within a reasonable distance of the ten surveys. Several synthetic traces were originally created using different sets of well logs from different deep boreholes in the surrounding region. The resulting synthetic traces were then empirically evaluated based on comparison with traces from the seismic data. The synthetic trace from two wells, Hudson #1 (IGWS ID:147749) and the Conn #1 (IGWS ID:134587) (Fig. 13), are deemed best able to match their synthetic to seismic sections.

Synthetic traces are produced using a sonic (transit time) log and a density log. In this case however, the well log data set associated with Hudson #1 only includes a sonic log. Consequently, the first step in the creation of that synthetic trace required the conversion of the available sonic log into a density log. The IHS Kingdom software converts transit time into a p-wave velocity log using the relationship between transit time and velocity shown in Equation 1. The Kingdom software package then produces an acoustic impedance log from which reflection coefficients are derived (Eqs. 2 and 3). Reflection coefficients are then convolved with a wavelet extracted from the data being modeled on a time and trace interval that features coherent reflections with minimal noise. Generally, the most suitable time interval for wavelet extraction with respect to

this study is 0.1 to 0.5s TWT. This interval encapsulates nearly all of the data sets laterally continuous reflections and is very seldom disrupted by excessive noise.

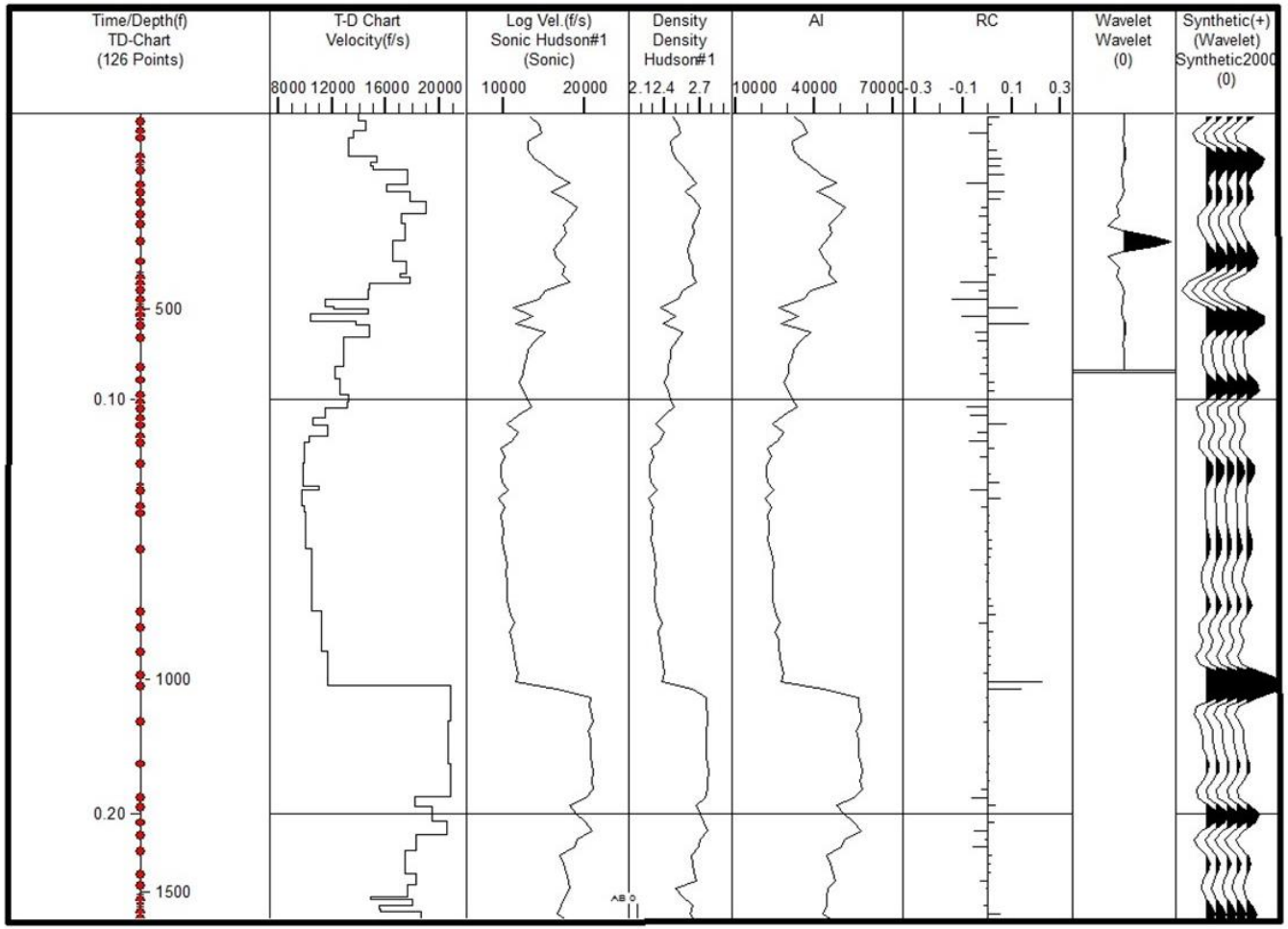

Equation 1

$$V_p = \frac{1{,}000{,}000}{transit\ time}$$

Equation 2

$$AI = V_p \times \rho$$

Equation 3

$$RC = \frac{AI_2 - AI_1}{AI_2 + AI_1}$$

Figure 12: Synthetic trace model produced from sonic log belonging to the Hudson well log dataset. Equation 1 describes how transit time, commonly measured in units of inverse velocity (micro-second per feet), is related to P-wave velocity (feet/second). Equation 2 is the relationship used to define the acoustic impedance of a point within a layer where V_p is the P-wave velocity and ρ is the density. Equation three derives the reflection coefficient which quantifies the contrast of acoustic impedance between two layers that relates to boundary reflectivity.

3.2.2 Regional Correlation Section

Correlation sections featuring major Paleozoic stratigraphic units are created for the purpose of evaluating whether or not it is appropriate to use data from distant deep boreholes for creating synthetic seismic models. This study constructs a correlation section using geophysical well logs, mud logs and driller observations from four deep boreholes in Indiana. Gamma ray, sonic and density logs are the primary geophysical log types implemented in this exercise. Sonic and density logs are generally able to easily establish the depth position of major stratigraphic boundaries. However, some units are not easily separated by density or transit time which is compensated for by the application of gamma ray interpretation. The four deep boreholes chosen for this task are Hudson #1 (IGSW ID:147749) located ~5 miles to the NE, Conn #1 (IGSW ID:134587) located ~25 miles to the NW, Peterson #1 (IGSW ID: 140431) located ~25 miles to the SW and Sherman #1 (IGSW ID:134161) located ~30 miles to the SE of the CountryMark dataset (Fig. 13). These wells are chosen specifically because they surround the field area and therefore give a good sense of the regional behavior of the Paleozoic stratigraphic variations. The data used in the creation of the resulting cross section is sourced from the Indiana Geological Survey's Petroleum Database Management System. The resulting correlation section demonstrates that using data from both Hudson #1 and Conn #1 is a viable option for creating synthetic seismic models. Though there is some inconsistency in the depth of each formation, the relative thickness between the top of the Trenton Limestone and the top of the Eau Claire Formation is generally uniform (Fig. 14). This in

combination with the dominant nature of the Trenton reflection, appears to allow the creation of a realistic synthetic to distances greater than that of Hudson #1.

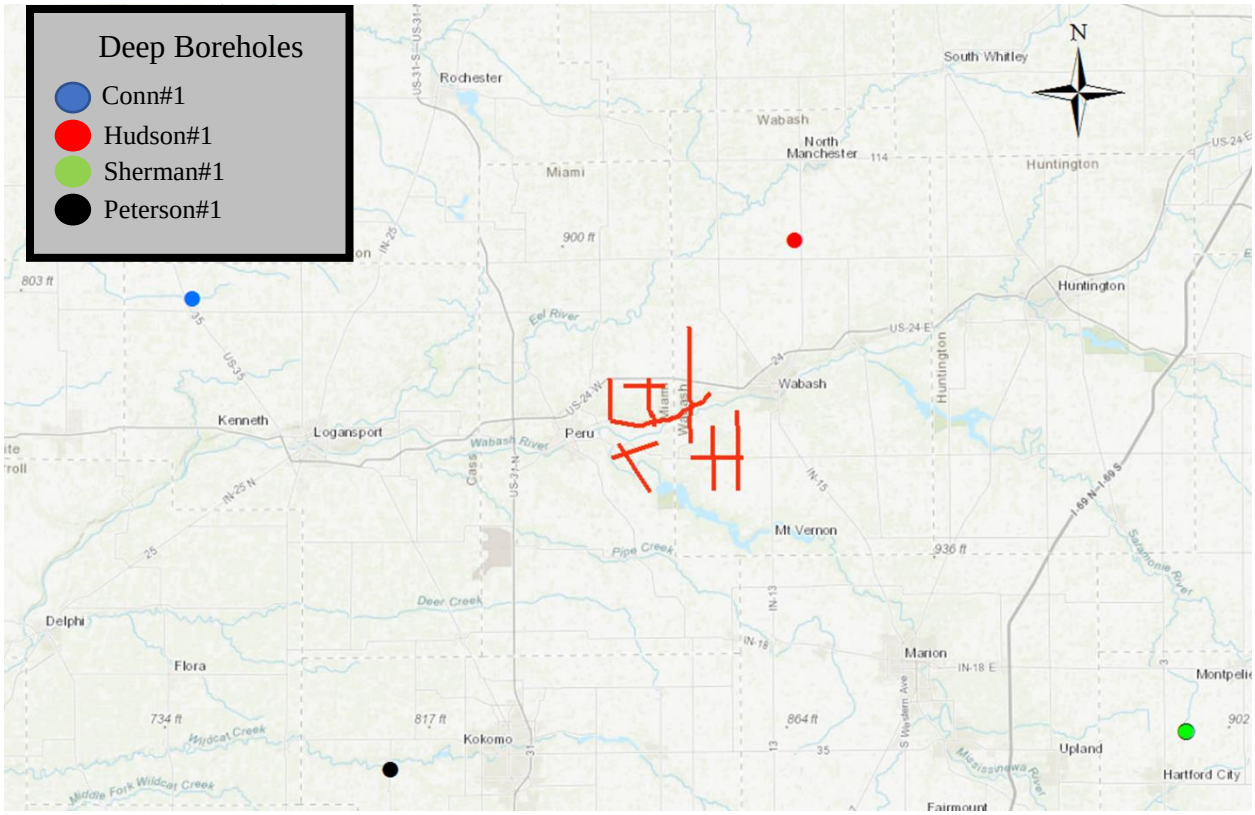

Figure 13: Location of wells incorporated into the interpretation of the Paleozoic stratigraphy overlying the area. Well logs from all four wells were incorporated into a regional correlation section. However, synthetic traces were formulated using well logs from Hudson#1 and Conn#1.

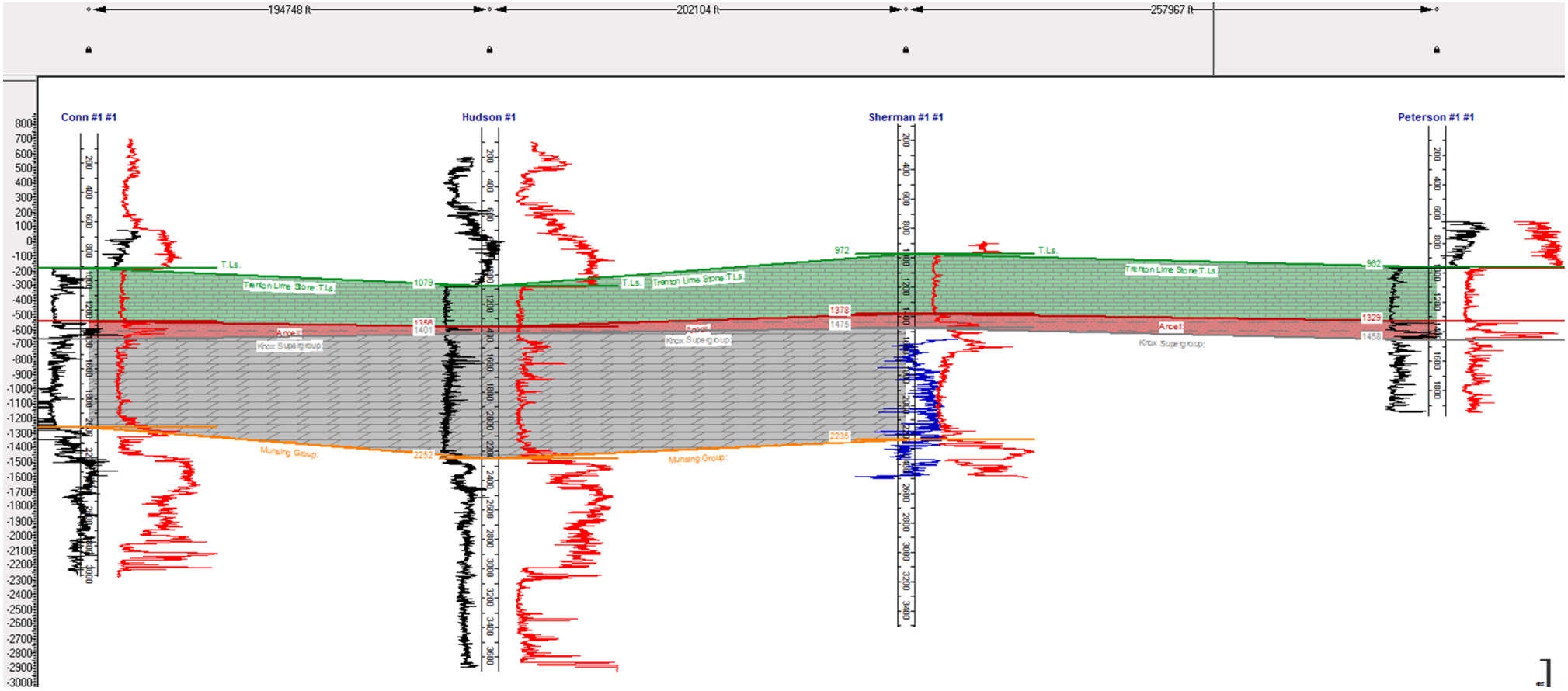

Figure 14: Regional trends of major Paleozoic sedimentary units as picked on geophysical well logs. These picks demonstrate that though some of the units that compose the interval from Munising to Trenton may thick and thin, the entire interval maintains a relatively uniform thickness. This allows us to adjust any synthetic from a regional deep borehole based upon the top of the Trenton Limestone and produce a synthetic trace with amplitude content indicative of the major Paleozoic reflectors.

3.3 Aeromagnetic Maps

3.3.1 Indiana Dataset

Residual aeromagnetic data is originally sourced from the Pan American Center for Earth & Environmental Studies (PACES) online gravity and magnetic database maintained by the University of Texas at El Paso (UTEP). The database is in the form of an online ArcGIS viewer application comprising three layers: a base map, an aeromagnetic data layer and a gravity data layer. The application utilizes a data extraction tool that allows the user to extract all data within a polygon drawn on the map. Data can be extracted in the form of a comma separated value text file (CSV) or in several other raster formats that are directly compatible with ESRI ARCGIS software. Most of the aeromagnetic data for the state of Indiana was gathered in 1947, 1948 and 1950 by the United States Geological Survey and the State of Indiana (Henderson and Zietz, 1958). Flight lines for this survey were gathered at a nominal 1 mile (1.6 km) spacing using an AN/ASQ-3A airborne magnetometer at an elevation of ~1000 ft (~305 m) above the ground (Henderson and Zietz, 1958).

This data set was first published in 1958 with the only compensation applied at that time being diurnal variation which was accomplished by the repetition of E-W baselines (Henderson and Zietz, 1958). The data were not reduced using the International Geomagnetic Reference Field (IGRF) until later when it was incorporated into the Ohio/Indiana/Illinois grid and subsequent national and international grid. A second statewide data set was gathered throughout the 1970's by the National Uranium Resource

Evaluation Program (NURE). The NURE program collected data in Indiana at an elevation of ~500 ft (~152 m) but with a flight line spacing of ~5 miles (~ 8 km). Aeromagnetic datasets acquired by the NURE program were commonly only crudely processed. This is primarily a product of reporting by contractors who were hired by the USGS with the focus of the study being placed upon airborne radiometric data. Diurnal variation was not always properly applied and commonly involved a method whereby the entire dataset was leveled to a single tie line (Hill, Kucks and Ravat, 2009). Inconsistencies in the individual residual magnetic grids were noted in later years when attempts were made to combine the grids for use in larger regional maps. This problem was solved by the development of the fourth iteration of a temporally continuous main field developed by the USGS (Hill, Kucks and Ravat, 2009). NURE data was used only for cross-comparison purposes and was not used for any interpretations made in this study.

3.3.2 Interpretational Filtering

The residual aeromagnetic dataset acquired from PACES is further filtered for interpretational purposes using the USGS DOS base potential field software package (Phillips, 1997). The software package being of considerable age requires grid file formats unlike the common Surfer, GEOSOFT, and ESRI formats that have become the modern standards. This makes creating grids within the software package an easier means of analysis rather than attempting to find a way to convert directly from ESRI, Geosoft or Golden Software formats. After gridding the data from an XYZ ASCII file using the USGS package program MINC, the data can generally be used in any of the other

modeling or filtering programs (Webring, 1981). It is suggested that the free format text file consist of three columns in the traditional XYZ ordering. It is also suggested that the data be exported as a tab delimited .txt format file where all XYZ values are expressed to the same number of digits. This study has primarily used the program FFTFIL, which transforms the magnitude of the data into a frequency equivalent via 2D fast Fourier transform (Hildenbrand, 1983). The program then convolves the frequency output with a filter/operator. The inputs of the operator are the unit wavenumbers of the spatial coordinates (Hildenbrand, 1983). Unit wavenumbers are calculated by convolving the spatial Nyquist frequency of the grid with the normalized wavenumber response.

3.4 Gravity Maps

3.4.1 Indiana Gravity Station Density

Gravity station density in Indiana is split into two different regimes. The southern portion of Indiana is represented by a station density suitable for large crustal scale observations; however, gravity station density in the northern portion of Indiana, where this study is located, is very sparse with only local dense grids. The density of data points in the study area is extremely sparse and are by themselves unsuitable for any in-depth analysis or interpretation. Consequently, a gravity survey was conducted as part of this study.

3.4.2 Gravity Data Acquisition

Gravity data acquisition for this study occurred over three days in early July and two additional days in mid-November, 2017. These trips were funded by the Benjamin

Richards Memorial Fund of the Wright State Foundation. Approximately 188 stations were occupied over the combined five days of acquisition (Fig. 15). Three of the 188 stations were used as base stations due to their convenient centralized location with respect to surrounding stations. Base stations were occupied approximately every hour for a total of 42 base station reoccupations. Gravity measurements were made using the LaCoste and Romberg gravity meter of Wright State University that has been recently updated with electronic levels. Many station locations were specifically chosen in order to target known seismic and aeromagnetic anomalies. Station locations were accurately surveyed using a Trimble 5800 receiver and TSC3 controller connected via cell phone wifi hot spot to the Trimble base station network in the region. Horizontal precisions were usually better than 0.05ft (1.5 cm) horizontally and 0.1ft (3 cm) vertically.

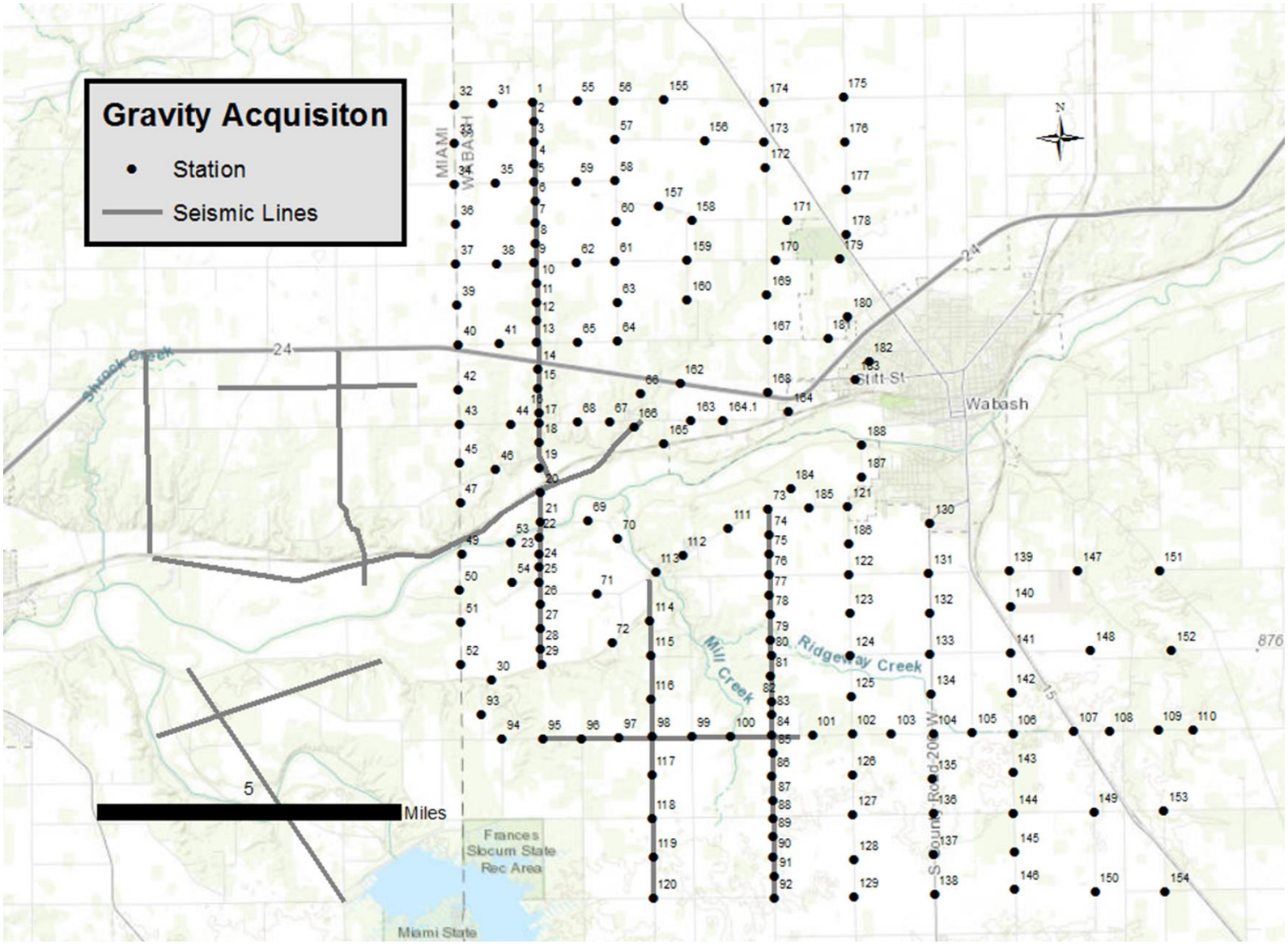

Figure 15: Station locations of the newly acquired gravity data set supported by the Benjamin Richard's Memorial Fund of the Wright State University Foundation.

3.4.3 Gravity Data Processing

Gravity data processing is conducted in three stages which are listed as chronological steps in Figure 16A. The first stage includes corrections that are the classical reductions for gravity data: tidal/instrumental drift, latitude, Free-air, Bouguer, and terrain corrections. The second stage involves a new correction to compensate for variation in bedrock topography. Stage three includes further reduction and filtering using the USGS potential field processing package.

The first processing step of gravity data is always correction for drift. By applying a drift correction, a geophysicist is compensating for measurement discrepancies caused by temporal changes in the environment (i.e., earth tides) as well as deviations caused by the mechanical and electrical systems of the instrument (Hinze et al., 2013). Solid earth tides are a major source of drift and are a natural phenomenon associated with the response of the Earth to the gravitational gradient over its volume exerted by the moon and Sun (Reynolds, 2011). Drift is measured via the regular reoccupation of a base station so that the drift can be monitored throughout the day (Fig. 16B). It is common practice for the base station to be occupied for measurement every hour. However, this time interval can be modified depending upon the magnitude and nonlinearity of the drift as observed by the acquisition team.

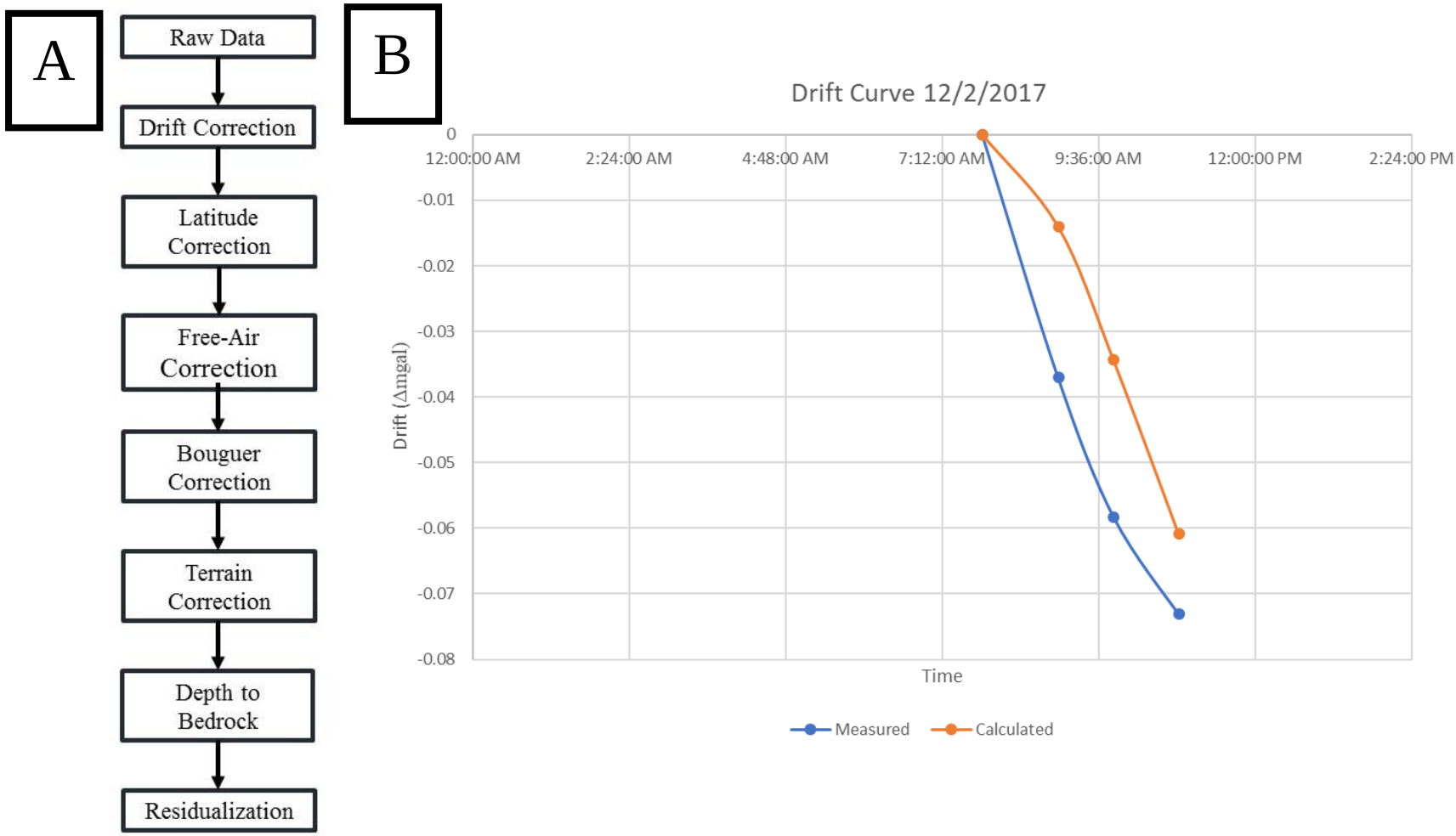

Figure 16: (A) Processing steps for newly acquired gravity data set primarily gathered along gathered in the NE quadrant of the study area. **(B)** Drift Curve created from base station measurements in order to account for instrumental and environmental noise.

Drift correction is followed by latitude correction. A latitude correction for a survey of this relatively small size is routinely derived by substituting the latitude of a datum station into Equation 4 to arrive at a correction factor in the units of milligals per kilometer (Hinze et al., 2013). Equation 4 is only a viable method for gravity surveys covering a limited area that are proximal to 45^{o} latitude (Hinze et al., 2013). The correction factor is then multiplied by the distance north or south of the datum point to produce a correction for each station in the units of milligals (mgal). The correction is then added if the station is located to the south of the datum or subtracted if the station is located to the north of the datum. The datum station for this survey is Station 37 which has a correction factor of ~.8$\frac{mgal}{km}$.

Equation 4: $$\frac{\Delta g\theta}{\Delta X_{N-S}} = 0.8144 * 10^{-3}\sin(2\theta)$$

The free-air correction is applied to compensate for elevation differences of the stations. Gravity decreases as elevation increases at a rate of ~0.3086 mgal per vertical meter or ~.01$\frac{mgal}{ft}$ (Hinze et al., 2013). This rate of change is commonly referred to as the free-air correction factor. Free-air correction is applied to this survey by defining Station 37 as a datum and multiplying the correction factor by the change in elevation for any given station (Eq. 5). The free-air correction only takes into account the variation in gravity due to the increase or decrease in elevation and doesn't take into account the

gravitational effect of the mass of the material that occupies the topography. The Bouguer correction compensates for this mass (Fig. 17) and is derived for any given station through the application of Equation 6 (Hinze et al, 2013) where G is the universal gravitational constant, δ is the density of the material that composes the elevation variation in $\frac{kg}{m^3}$, and h is the actual variation in elevation measured in meters. It should be noted that G in Equation 6 has been scaled in order to derive output values in the units of milligals. For this study we implement a density of $1800\frac{kg}{m^3}$ because the near surface material is composed of glacial till, sand, and gravel. The resulting gravity value after application of the Bouguer correction is referred to as the Bouguer anomaly.

Equation 5: $Correction\ mgal = (Z_{station-}Z_{37})m * .3086\frac{mgal}{m}$

Equation 6: $Correction\ mgal = 2\pi G\delta h = (4.193 * 10^{-5}) * \delta * (Z_{Station} - Z_h)m$

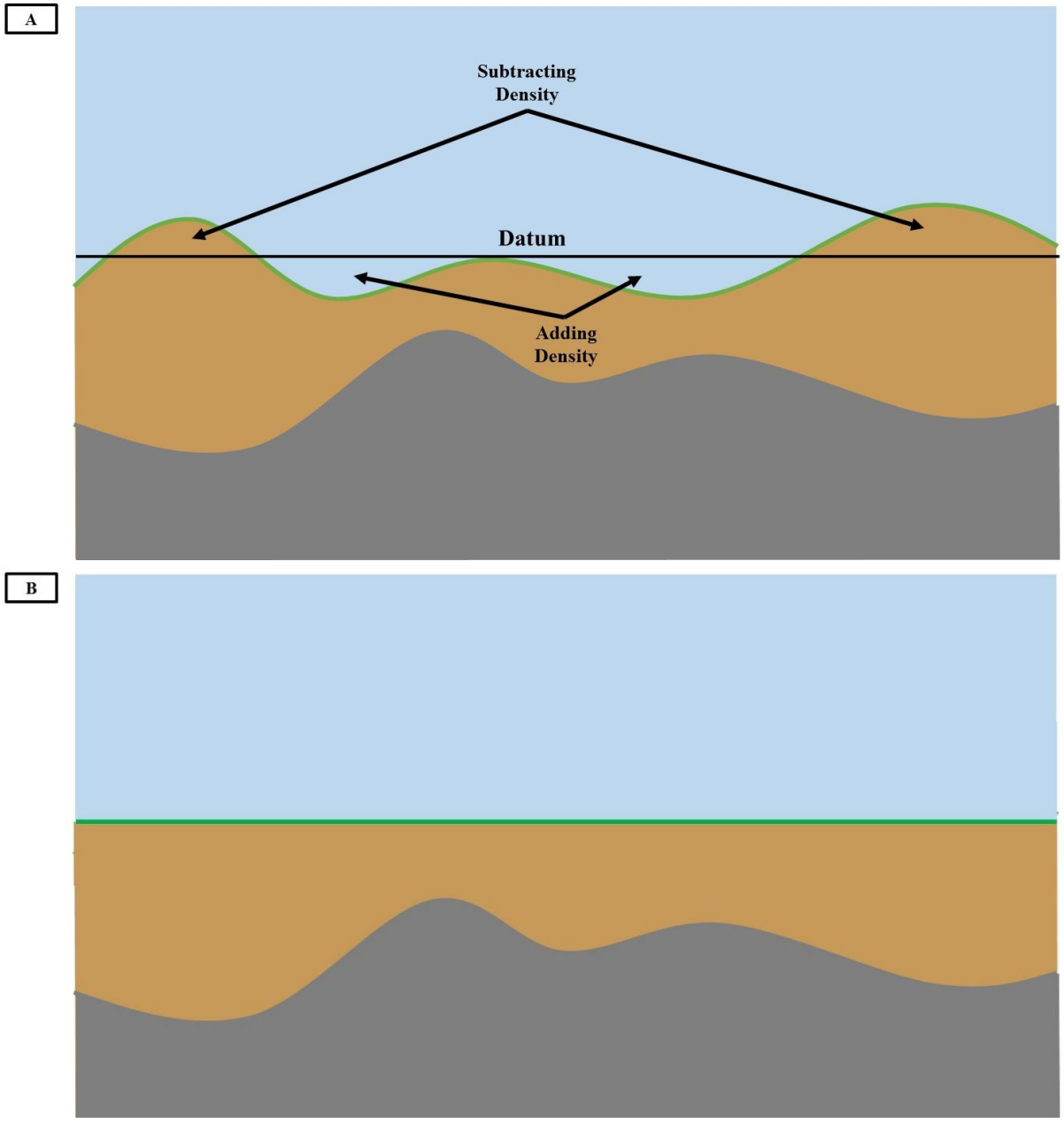

Figure 17: (A) Topography that represents the status of gravity measurements prior to the application of the Bouguer reduction which places all stations at an equal datum underlain by unconsolidated sediments. **(B)** Status of the plane to which gravity measurements are reduced after the application of Bouguer reduction. Technically, this is a depiction of the plane after both Bouguer and terrain corrections.

Terrain correction is usually the final reduction applied to gravity data sets. Terrain corrections are applied to adjust the Bouguer correction for topographic variations in the surrounding area (Reynolds, 2011). Terrain corrections have historically been carried out using Sigmund Hammer's classical methodology (Hammer, 1939). For this study however, we employ the aid of computers by using a program developed by Dr. Doyle Watts that makes use of digital elevation models (DEM) and survey data to approximate terrain correction factors. Here, I employ DEMs sourced from the Indiana Spatial Data Portal (ISDP, 2018) and the high precision surveying capabilities of modern GPS systems. Tentative terrain correction factors calculated by the program are multiplied by ~0.006 and the Bouguer density in order to derive the final correction factor. After completing terrain corrections, the data is commonly referred to as the Terrain Corrected Bouguer anomaly, or the complete Bouguer anomaly.

3.4.4 Correction for Depth to Bedrock

Just as gravity measurements are sensitive to elevation and the mass contrast due to topography, gravity measurements are also sensitive to variation in bedrock elevation. This poses a significant problem for this study's gravity data set as the bedrock depth in the area ranges from ~2 ft (~0.6 m) to 200+ ft (~61+ m) and the goal of this study is to observe gravity magnitude variations that are a product of geologic structures within the Precambrian rocks at depth. This study approaches this problem using a modified version of the Bouguer correction that employs finite difference grids (Fig. 18). The grids required for this method include an equal source grid that represents an infinite plane based on the maximum bedrock elevation, an equal source grid that represents the

Bouguer constant derived earlier through the application of Equation 6, a grid that represents the variation in bedrock elevation, and a grid of the complete Bouguer anomaly. The following three-step method using simple grid algebra is then employed: (1) The bedrock elevation grid is subtracted from the equal source grid representing the infinite plane based off of the maximum bedrock elevation. (2) The resulting grid is then multiplied by the grid representing the Bouguer constant. (3) This grid should be indicative of the loss in gravity due to increased bedrock depth and is therefore added to the gridded complete Bouguer anomaly data. A density contrast between glacial drift and bedrock of 0.7 $\frac{g}{cc}$ is used.

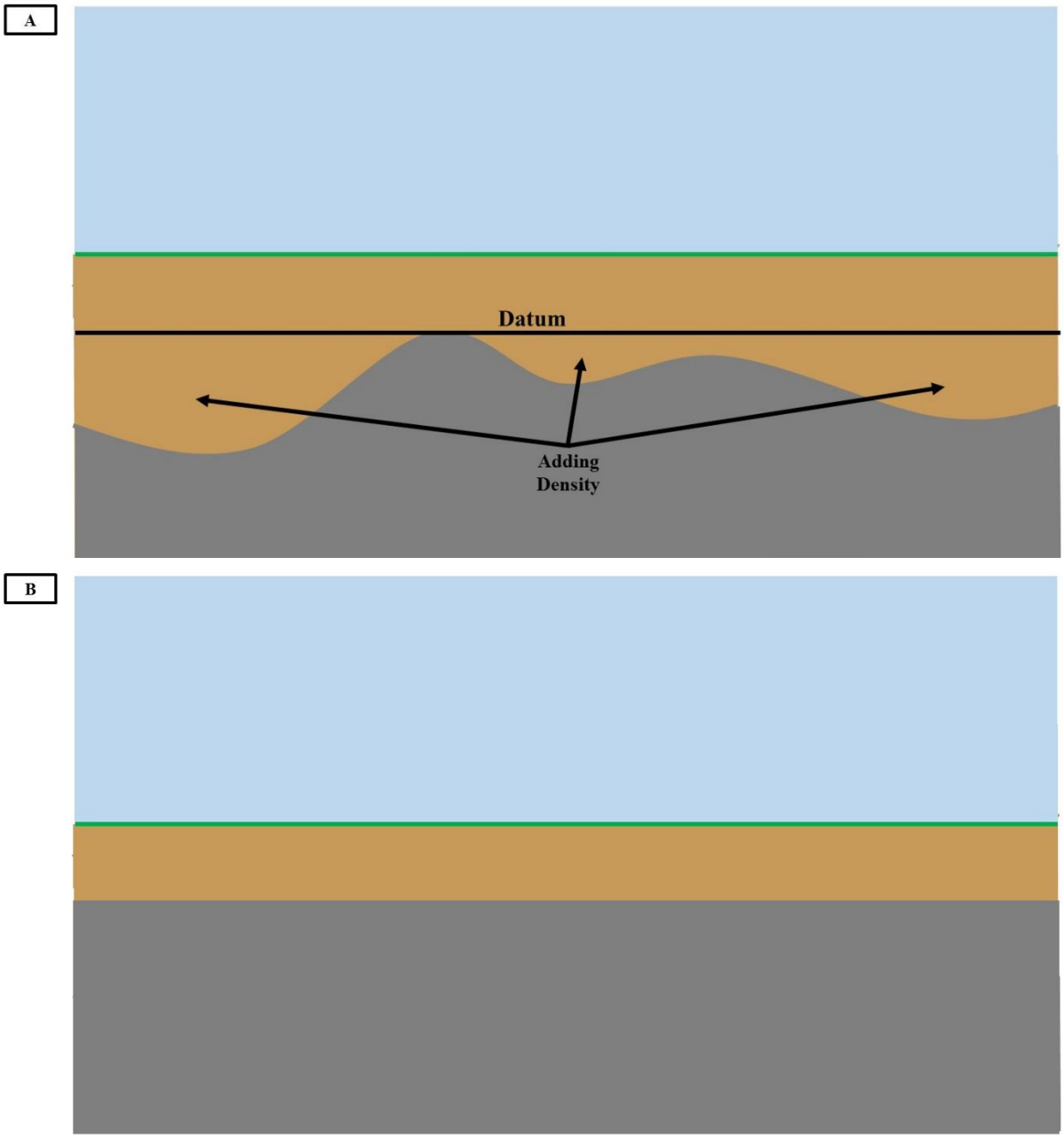

Figure 18: (A) Status of the plane the gravity measurement sits upon after Bouguer and terrain corrections prior to the application of a pseudo-Bouguer correction for variation in depth to bedrock. **(B)** Status of the bedrock plain after reduction for the variation in depth to bedrock.

3.4.5 Residual Gravity

I applied a final processing step to the newly collected gravity data set to remove the regional gravity field. The regional field can in many cases be estimated using low order analytical functions (Telford et al., 1990). This largely depends on the size of the study and the general complexity of the survey areas gravity field after reduction to the Bouguer anomaly. This study used the program SURFIT that is a part of the USGS potential field software package. SURFIT fits orthogonal polynomials of up to the 19^{th} order to achieve an estimation of the regional field (Branch of Geophysics, 1989). After deducing the regional field, the program then subtracts the trend of the regional field from the gridded data and produces a grid of the local gravity anomalies. The regional field should be estimated by very low order polynomials of no greater than the 3^{rd} order due to the limited sized of the survey. Application of this correction, though typical a crucial step in processing, proves to be unnecessary as a good approximation cannot be determined due to the limited size and high-resolution nature of the data set.

3.5 Depth to Bedrock Data

A gridded elevation map of the bedrock is created for gravity reduction purposes. Sources of data for this map include reports of depth to bedrock compiled from the Indiana water well database from the Indiana Department of Natural Resources and values for depth to bedrock gathered for this study by applying horizontal over vertical spectral ratio (HVSR) analysis to three component passive seismic data acquired using a TROMINO, an instrument developed by MOHO Science & Technology in Italy. The

HVSR method uses ambient seismic noise to determine a fundamental resonant frequency (Lane et al., 2008). The frequency is determined through analysis of the spectral ratios belonging to the horizontal and vertical seismic components measured by the three component TROMINO instrument (Lane et al., 2008). Software is generally used to synthesize results in a diagram that quantifies the horizontal/vertical spectral ratio for the given station location (Fig. 19). When applied to a simple two-layer model where the resonant frequency refers to that of layer 1, equation seven applies. Equation 7 can be rearranged to calculate the thickness (Z) of layer one where f is the fundamental frequency, and V_s is the shear wave velocity. This method is generally best applied when V_s is first determined by occupying a station with a nearby water well where the value of Z is already known.

Equation 7: $f = \frac{V_s}{4Z}$

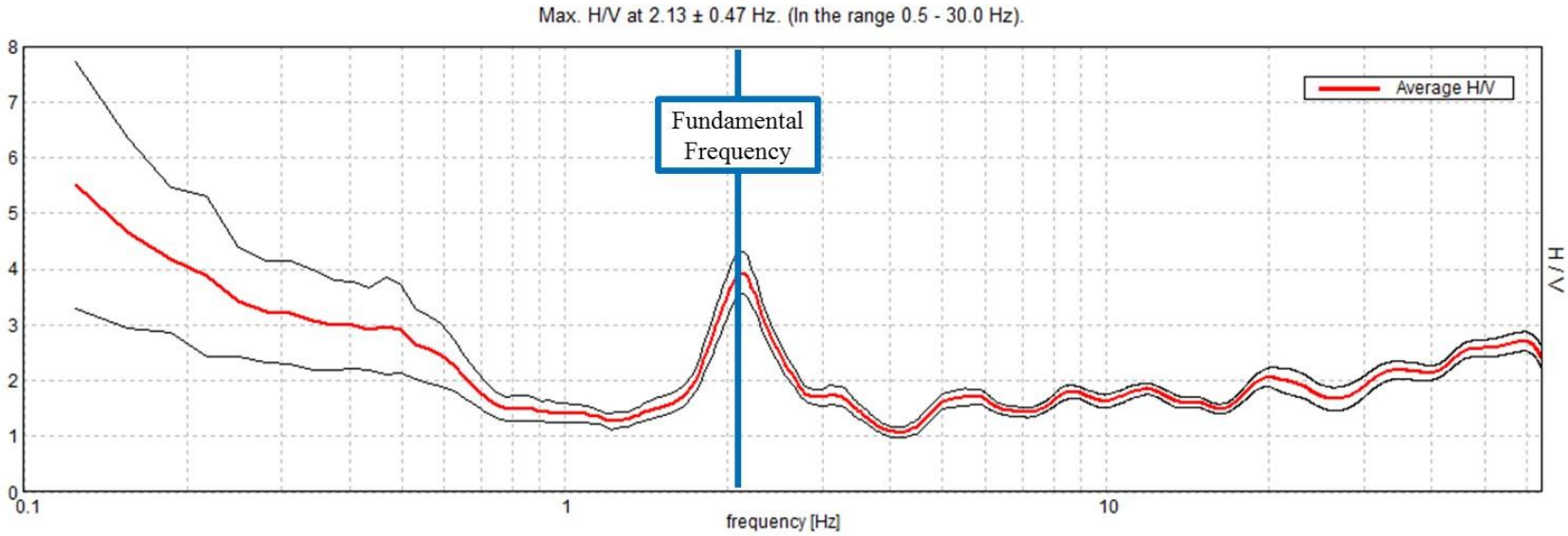

Figure 19: H:V spectral ratio graph produced by MOHO's software package Grilla. The fundamental frequency interpreted to represent the layer associated with the thickness of unconsolidated sediments is picked using the blue line.

4.0 Discussion

4.1 Seismic Interpretation

4.1.1 General Interpretation

The ten seismic sections can be characterized by three different seismic intervals or zones separable by their variations in acoustic response. Figure 20 outlines these three distinct intervals and refers to them as Zones A, B and C. Zone A is characterized by mostly flat-lying reflectors down to ~0.5 s TWT. The reflectors of Zone A are present on all ten seismic sections and can be tied from one section to the next with little to no mis-tie. Zone B is the beginning of the Precambrian seismic interval and is separated from Zone A by the Precambrian unconformity. Zone B is characterized by little to no internal seismic response and generally continues undisturbed for ~1.0 s TWT. Zone C is the portion of the Precambrian interval characterized by seismic response in the form of discontinuous reflections and diffractions. Zone C will also be referred as the internal Precambrian seismic interval and is not present on all of the seismic sections.

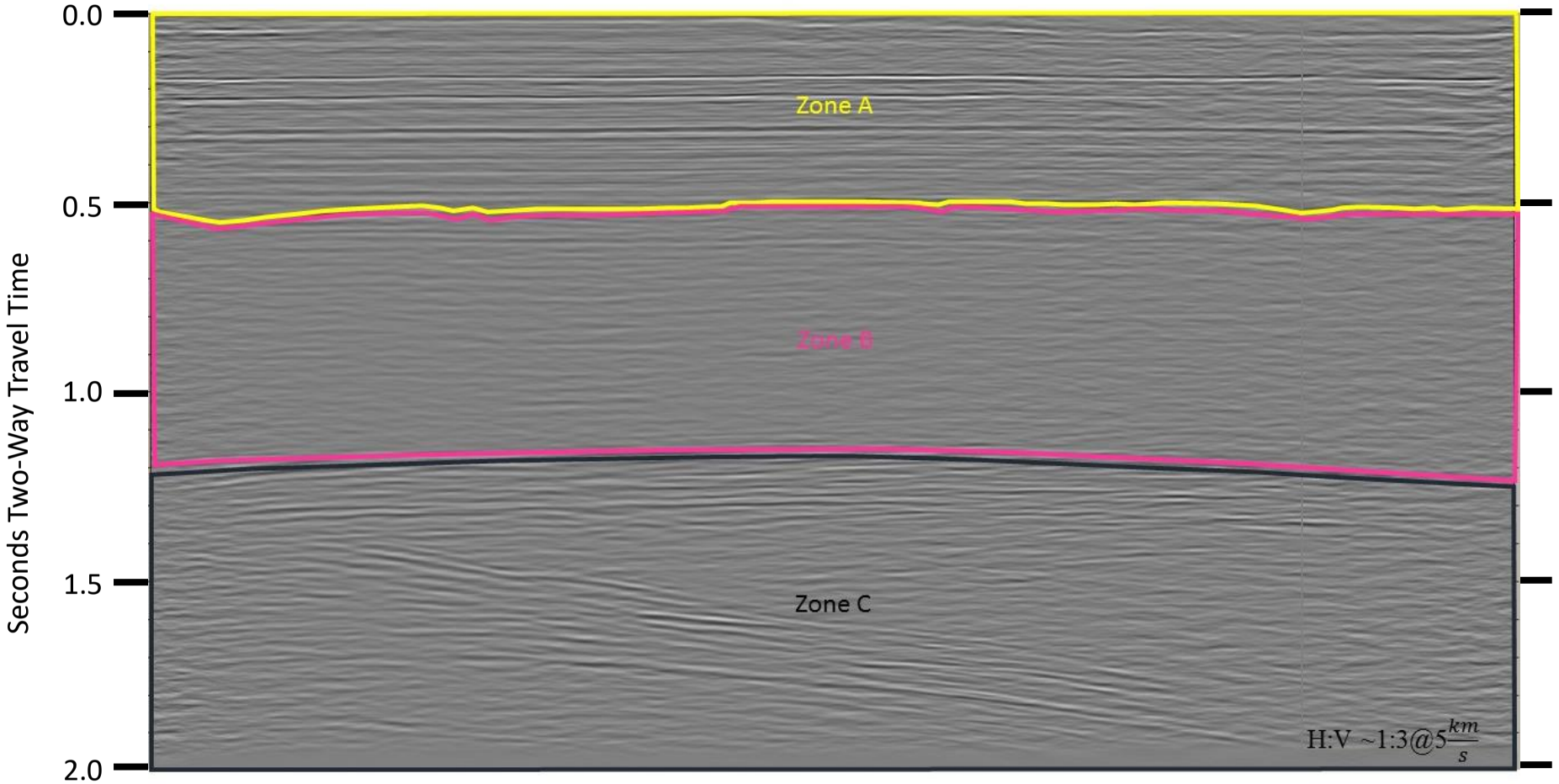

Figure 20: Broad generalization of the three different zones of seismic character observable on the seismic data set examined by this study. Zone A is composed of generally flat and layered reflectors, Zone B is composed of a massive interval with little to no acoustic response, and Zone C is composed of incoherent and broadly arching reflections and diffractions.

4.1.2 Interpretation of Paleozoic Interval

Major Paleozoic reflectors include the top of the Trenton Limestone, the top of the Knox Supergroup, the top of the Eau Claire Formation and the top of the Mount Simon Sandstone (Fig. 21). The top of the Trenton Limestone is represented by a high amplitude positive reflection that occurs at ~0.18 s TWT (Figs. 21 and 22). The top of the Knox Supergroup is a well-known regional unconformity and is interpreted here to be represented by the undulating reflection positioned directly above the top of the Potossi Dolomite. The top of the Knox Supergroup is intermittently disturbed by thin bed tuning caused by erosional remnants belonging to the St.Peter Sandstone which is likely the only surviving unit of the Ancell Group. The top of the Mount Simon Sandstone is difficult to separate from the several alternating reflections belonging to the Eau Claire Formation using only the character of the sonic log. This is a result of the gradational nature of the boundary between the Eau Claire Formation and the Mount Simon Sandstone in the region. This gradational character, as demonstrated by the wire line logs in Fig. 21, reduces the large acoustical impedance boundary that is commonly observable in parts of the Illinois Basin. For this reason, I heavily rely on the gamma ray log from Hudson #1 to help distinguish between the top of the Mount Simon Sandstone and other similar reflections belonging to the overlying Eau Claire formation (Fig. 21). The use of a gamma ray log is a viable option in this case because the Mount Simon Sandstone is composed of predominately quartz sandstone with a significantly lesser proportion of shale than the Eau Claire Formation. This suggests that the gamma signature of the Mount Simon Sandstone

should be lower and have low variability in comparison to that of the Eau Claire Formation (Fig. 21).

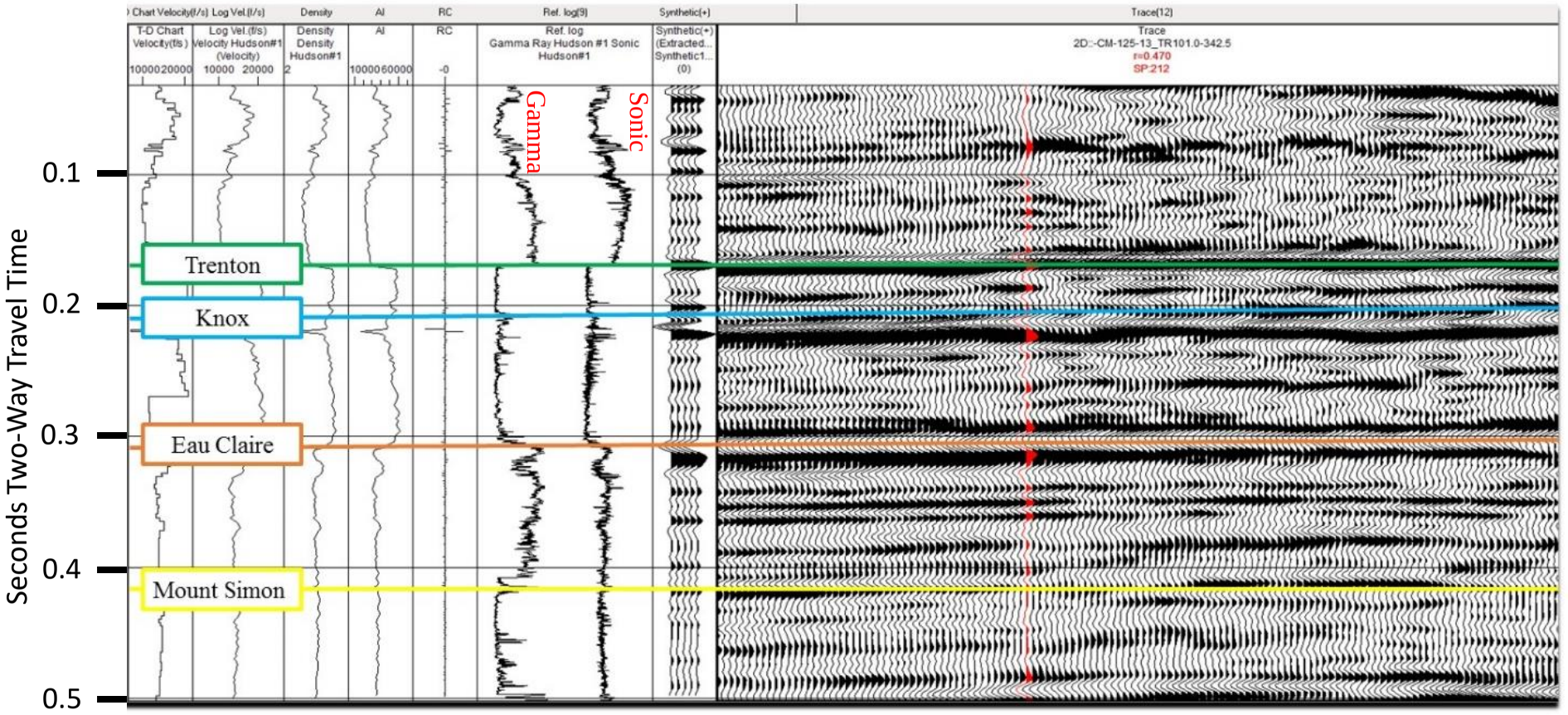

Figure 21: (A) Synthetic correlation of Paleozoic reflectors using traces from east facing line CM-125 using the wire line log data set from the deeply penetrating well, Hudson #1. **(B)** Interpreted section CM-125.

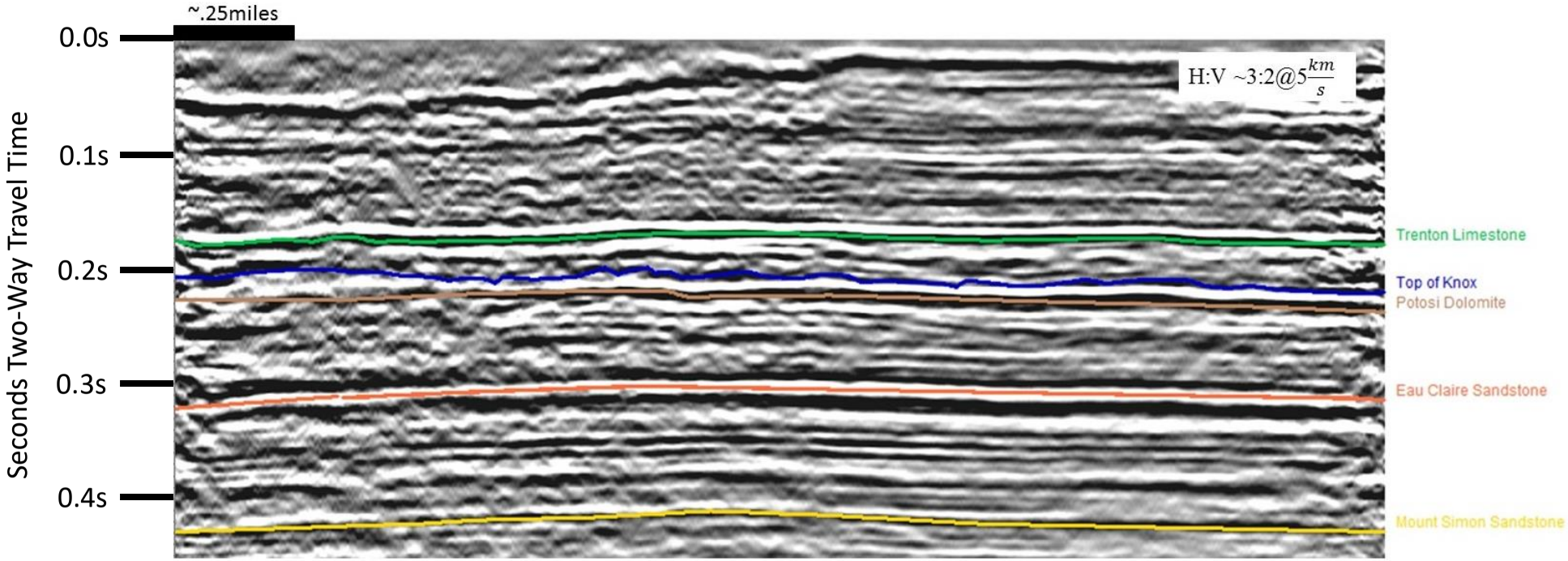

Figure 22: Major Paleozoic reflectors picked on line CM-125. These units include, in ascending order, Mount Simon Sandstone, Eau Claire Sandstone, the Potosi Dolomite, the top of Knox, and the Trenton Limestone.

4.1.3 The Precambrian Unconformity

The Precambrian unconformity occurs at ~0.5 s TWT on all ten of the seismic sections. It is characterized by undulations, bowtie artifacts and accompanying diffractions. These observations indicate that the Precambrian Unconformity underlying this locality of the EGRP is a surface of high relief (Fig. 23). This characterization of the Precambrian unconformity is reminiscent of the topography of the St. Francois Mountains of SE Missouri, but the analogy has never been applied to the interpretation of the Precambrian unconformity in other regional seismic reflection studies of the EGRP. Other seismic studies have reported the Precambrian unconformity within the bounds of the EGRP to be mostly smooth and flat or slightly dipping. Many have observed layering, suggesting that the underlying lithologies are likely Precambrian sequences of sedimentary or volcanoclastic origin (Pratt et al. 1992; Drahovzal, 1997; McBride et al., 2016; Peterman, 2016; Parent; 2017). The presence of classic seismic artifacts indicating a surface of high relief is how the Precambrian unconformity on unmigrated seismic sections is here interpreted. The processing step of migration aims to removing or smooth bowtie artifacts and diffractions; however, the migration of what is very much a 3-D structure on a 2-D section does not reconstruct the real structure since out of plane reflections can be smeared into incorrect locations. Precambrian unconformity topography expressed on the ten seismic sections is difficult to quantify given the general nature of crustal scale seismic reflection data and the lack of 3D coverage. This is why this study implements zero-offset ray-trace modeling of actual profiles of the EGRP paleo-topography expressed in the St. Francois Mountains for comparison with the 2D

seismic profiles. Fig. 24 is an example of one such model developed from a cross section that cuts across the subvolcanic granite terrane of the EGRP in the St. Francois Mountains. This model features the same seismic characteristics that are observable on the ten stacked seismic sections, demonstrating that the Precambrian unconformity of this study reasonably compares with that seen in the St. Francois Mountains.

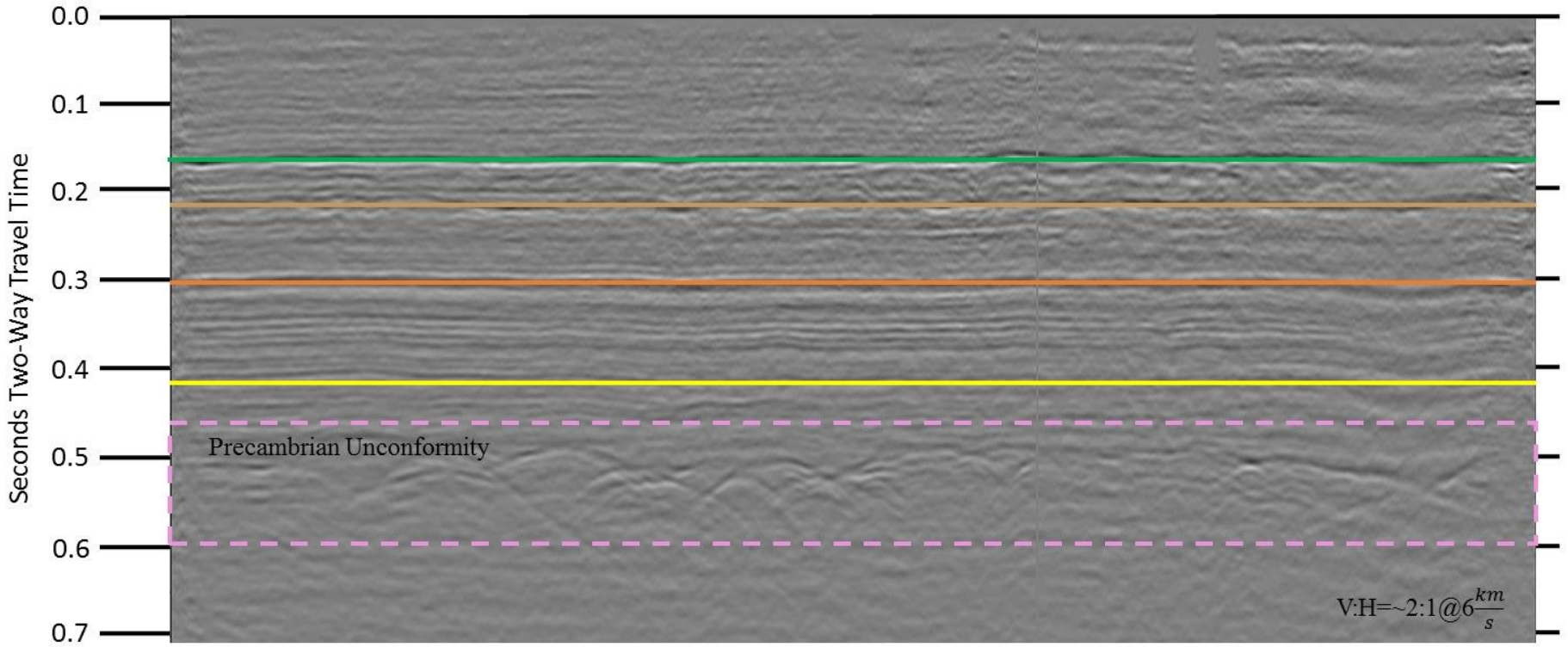

Figure 23: The Precambrian unconformity as observed on the stacked seismic section CM-127. The seismic character of the Precambrian unconformity shared by all ten of the seismic sections. The character of the Precambrian unconformity includes undulations, bowtie structures, and diffractions all of which are indicative of a surface of high relief.

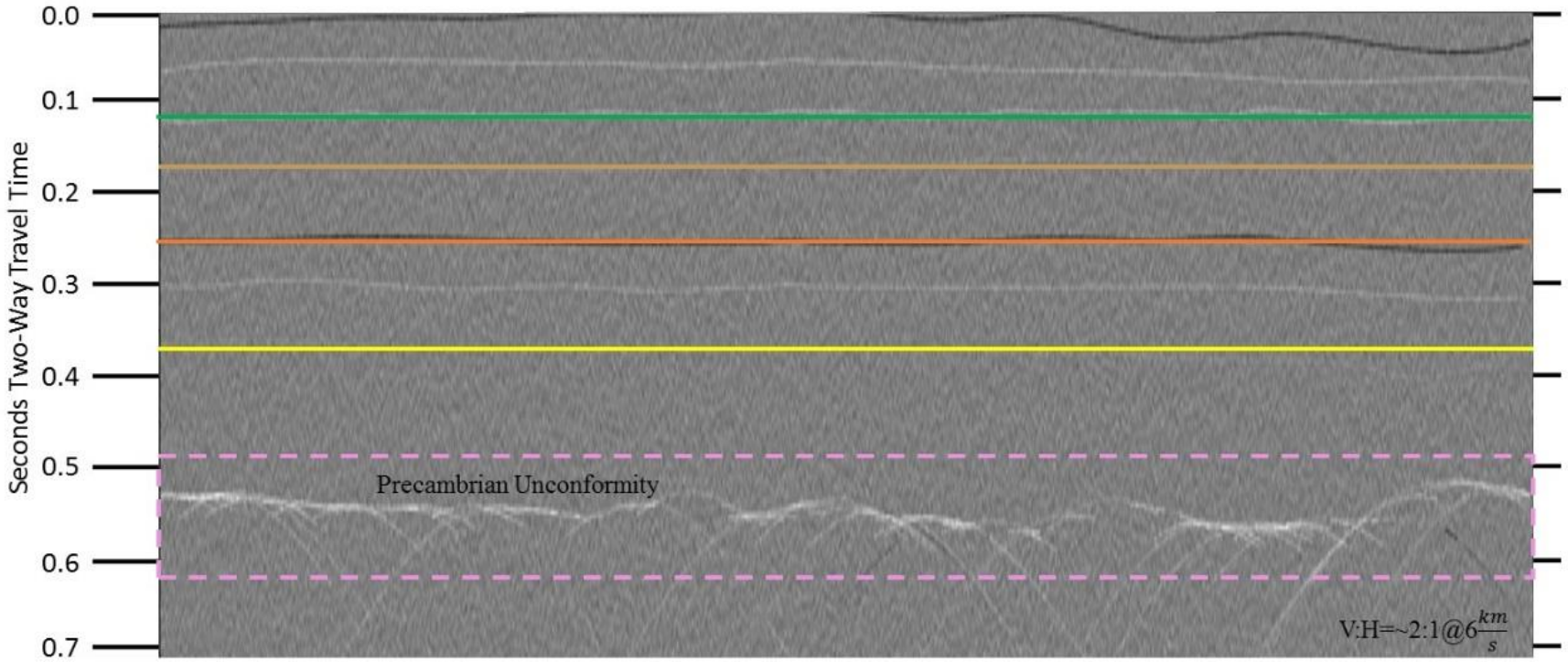

Figure 24: Modeled section using profile extracted across the St. Francois Mountains subvolcanic granite terrain. This model was produced using parameters aimed at producing the closest virtual simulation of what would have been produced during the acquisition of CM-127. This model demonstrates that the seismic character of the Precambrian unconformity as observed on CM-127 is indeed indicative of a surface of high relief.

4.1.4 The Precambrian Interval

The Precambrian interval is divided into two zones which feature very different seismic characteristics. Zone B represents the uppermost portion of the Precambrian interval underlying the Precambrian unconformity. It is characterized by a lack of acoustic contrast response and is therefore interpreted to be a massive zone of EGRP granite with a likely approximate age of between ~1.45-1.27 Ga (Bickford et al., 2015) as encountered in drill holes in the nearby region such as Hudson #1 and Conn #1 (Fig. 12). EGRP granite samples from these two boreholes are the only constraining data locations for the Sm-Nd model line determined by Bickford et al. (2015) within the north-central portion of Indiana. This broad range of ages makes correlating the emplacement of Zone B with either the earlier or later stages of EGRP development difficult without more geochronological and petrographic constraints. However, additional provenance data from core samples gathered from deep boreholes to the E and NE in Ohio and Michigan allow us to reasonably constrain the age of the granite underlying the area to no later than ~1.27 Ga.

Zone B is abruptly interrupted to some degree in all of the seismic lines by the occurrence of mostly discontinuous high-amplitude reflections and diffractions in what is here called Zone C. These strong reflections are generally present in the sections at ~1.5 s TWT or greater and are interpreted to represent an intrusive complex that likely consists of denser magmatic material emplaced at the same time as or not long after the development of the overlying granitic material. Lack of borehole penetration leads this study to rely upon other geophysical methods to develop a reasonable idea of what the

reflections of Zone C may represent. Specifically, I draw upon the newly collected gravity data set and publicly available aeromagnetic data set in order to develop a viable explanation.

The top of Zone C on seismic line CM-127 is represented by a slightly arcuate reflector that is truncated by a diffraction at the beginning of the northern 1/3 of the section (Fig. 25). Zero offset ray trace models of this zone indicate that the specific diffraction pattern associated with the truncation of the reflection is indicative of a thin horizontal body that is best represented by a thin sill (Fig. 26). Indications include two well developed sets of diffractions that occur at the termination. The first set move out to the north while the second set moves out to the south. Other representations of Zone C visible on CM-127 occur as arching zones of diffractions or interlayered reflections and diffractions. These small chaotic anomalies are reminiscent of features described as mafic plugs by McBride et al. (2016) (Fig. 27A) and of models describing interlayered mafic sills developed by Litak and Hauser (1992) (Fig. 27B). Additionally, the reflectors may represent intrusions associated with a multiphase intrusive ring-dyke complex. Seismic expressions of anomalies representing Zone C as seen and described on CM-127 are generally shared throughout the remainder of the seismic reflection data set.

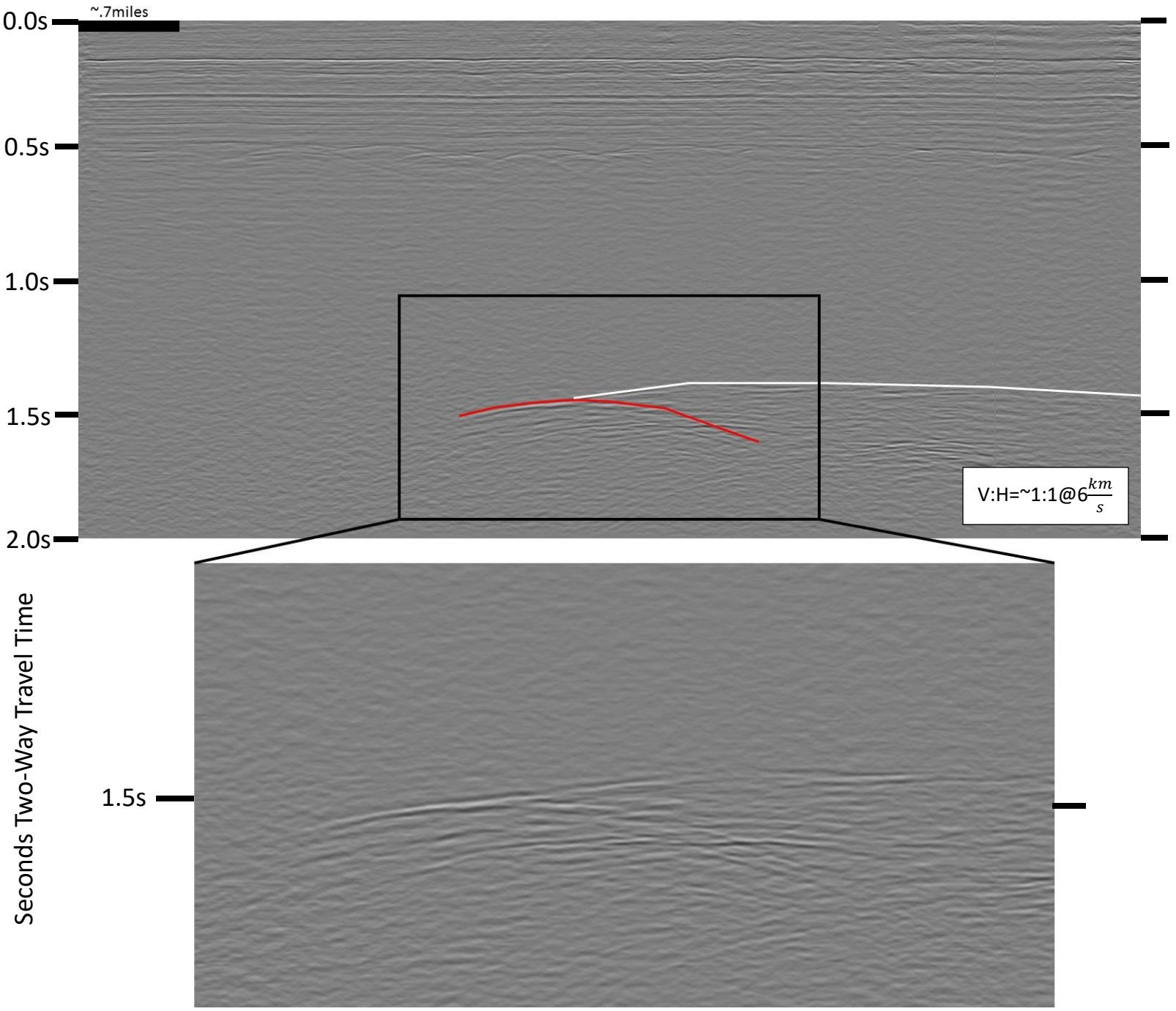

Figure 25: Eastward facing view of seismic section CM-127. The reflector interpreted to be the top of the internal Precambrian interval is traced in white. The traced reflection terminates at the beginning of the most northern third of the seismic section. The reflection termination is demarcated by a very distinct diffraction pattern which includes a northern bound and southern bound diffraction. The diffraction is traced in red.

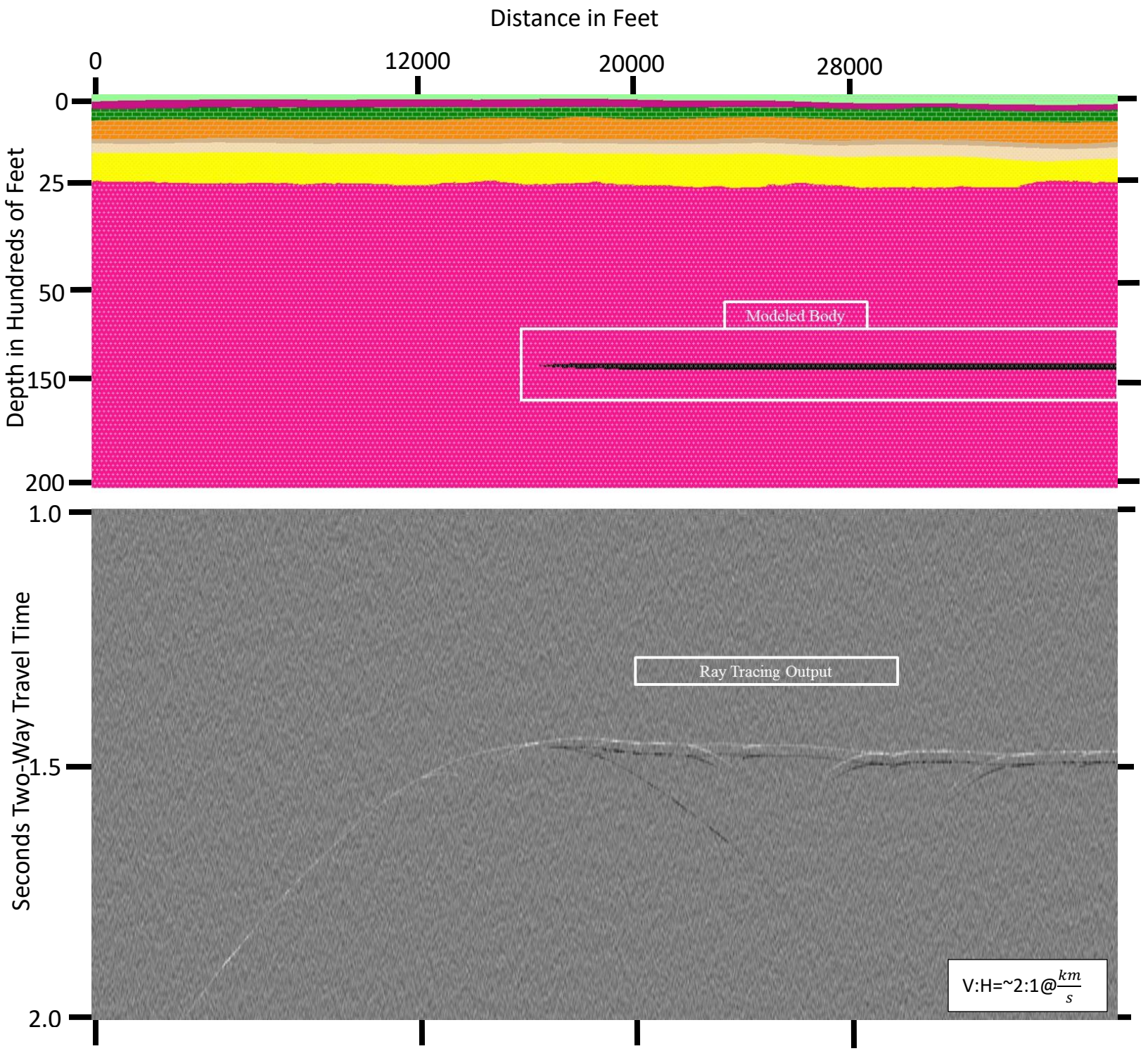

Figure 26: Zero offset ray-trace model of CM-127 constructed using Ion Geophysical's GXII 2D ray tracing software. Models indicate that the diffraction pattern observed at the termination of the internal Precambrian intervals uppermost prominent reflector is comparable with a diffraction pattern that would observed of a thin sill.

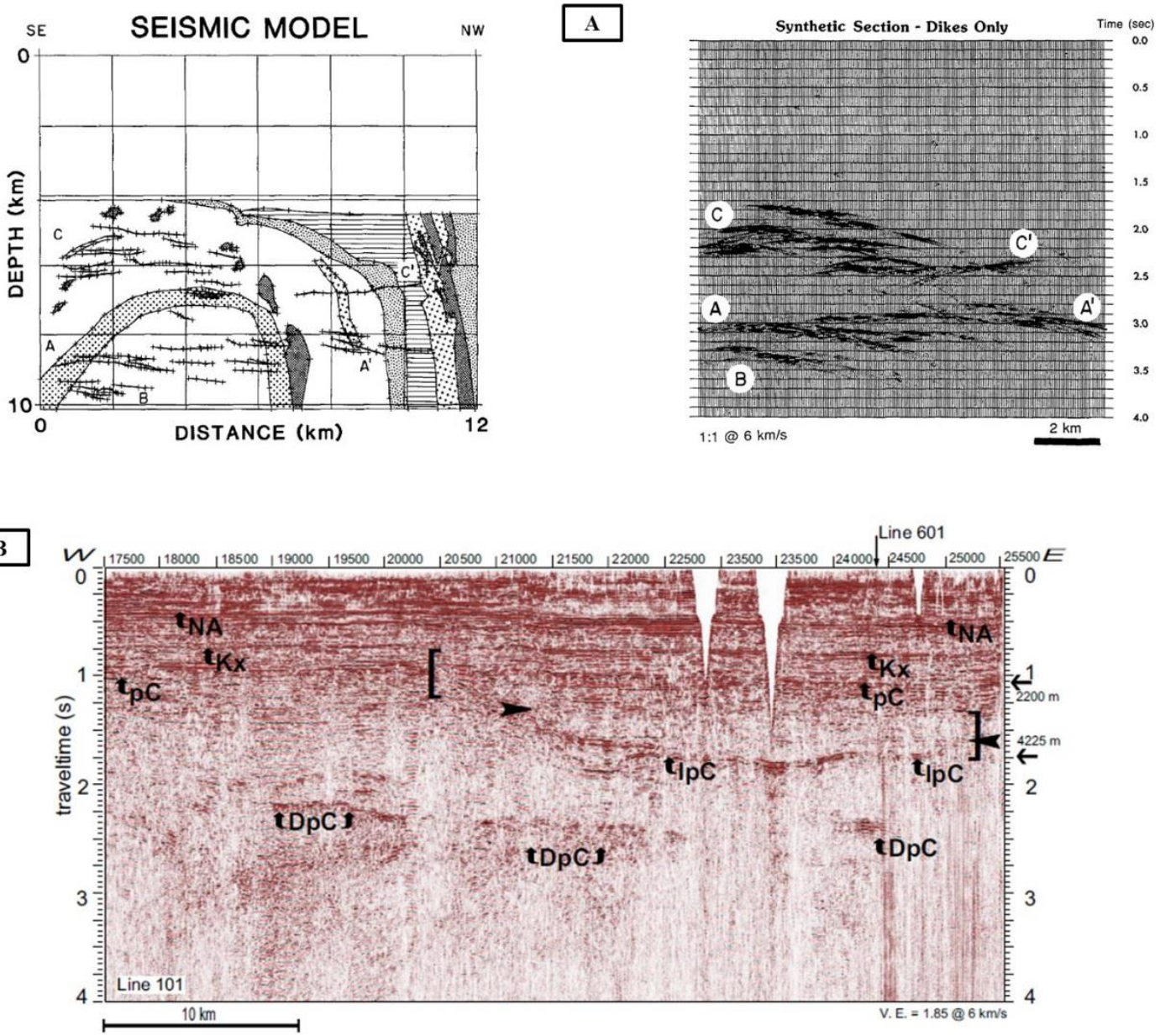

Figure 27: (A) Models of mafic sills used for interpretational comparison of the Bagdad Reflective Sequence identified to be part of the upper crust underlying Arizona by the COCORP project. (Modified from Litack and Hauser, 1992). Models were created by placing mafic sills observed at the surface in the Buck Mountains at depth (Litack and Hauser, 1992). **(B)** McBride et al.'s 2016 Precambrian interval interpretation of a long seismic line collected over the EGRP in Illinois (Modified from McBride et al., 2016). Ipc stands for the intra-Precambrian reflector interpreted by McBride et al. to likely be indicative of a bowl shaped sill complex. DPc stands for deep Precambrian reflective/diffractive zones interpreted to be mafic plugs or isolated sills.

The other nine seismic sections display very similar expressions of the internal Precambrian interval (Zone C) as those observed on CM-127. CM-198 is an E-W seismic line ~2 miles to the west of N-S line CM-127. Zone C is predominately expressed on CM-198 as very coherent reflections that gently dip to the east (Fig. 28). Above these gently dipping reflections are arching reflections that appear to form a bow-tie artifact on the east-central portion of the time section. There is uncertainty in whether or not the arcuate reflections observed on CM-198 are real structures or side swipes as the features are not observed on the northern portion the crossing line CM-174 (Fig. 29). CM-182 and CM-162 are crossing lines located in the SW corner of the seismic survey area. The internal Precambrian interval on the two stacked time sections is represented by an arching zone of reflections that drape off the bottom (Fig 30). CM-130 ,131, and 158 are crossing seismic lines that are located in the SE portion of the survey area. CM-130 and 131 share very similar expressions that emulate broader and more shallow expressions as seen on CM-182 and 162 (Fig. 31). Reflections on CM-130 and 131 appear to be nearly identical and may be tied to CM-158. Seismic line CM-158 features a flatter expression of the internal Precambrian interval (Fig. 31). Reflections observable on CM-158 do not drape off the bottom, but appear to terminate near the eastern edge of the section. It is difficult to determine whether or not the termination of the reflectors on CM-158 is real geological change or perhaps due to low fold of coverage approaching the end of the seismic line. The internal Precambrian interval (Zone C) expressed on CM-138 is very complex and contains a set of reflections that apparently dip to the east and another set that arch to the west (Fig.32). The two sets of reflectors meet and form a bowtie artifact

near the center of the section. These two sets can both be tied to other cross lines and are therefore are thought to be real and largely within the plane.

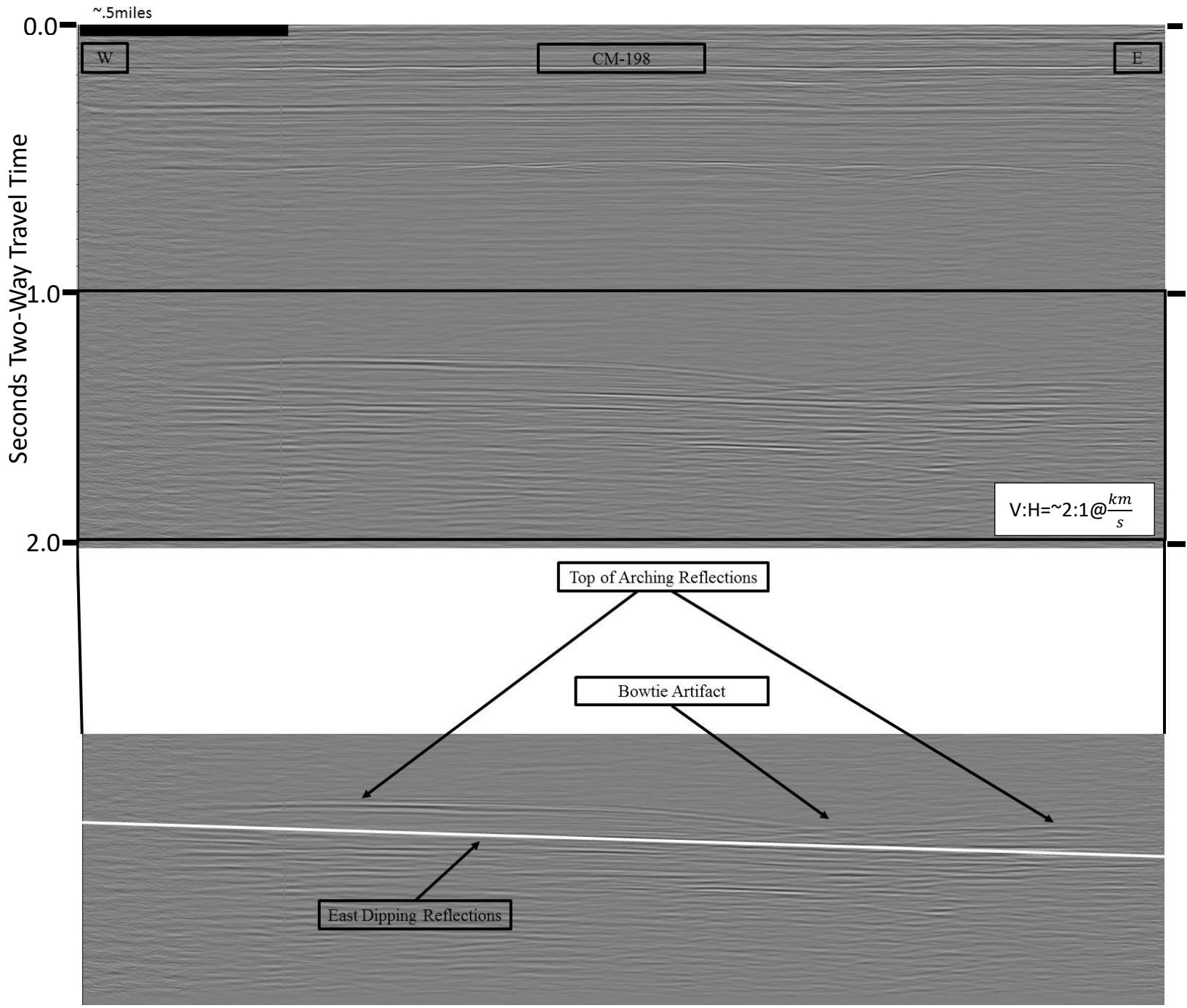

Figure 28: Seismic line CM-198 viewed toward the north. Internal Precambrian features include gently sloped reflectors that apparently dip to the east and arching reflectors that are observable above the gently sloped reflectors.

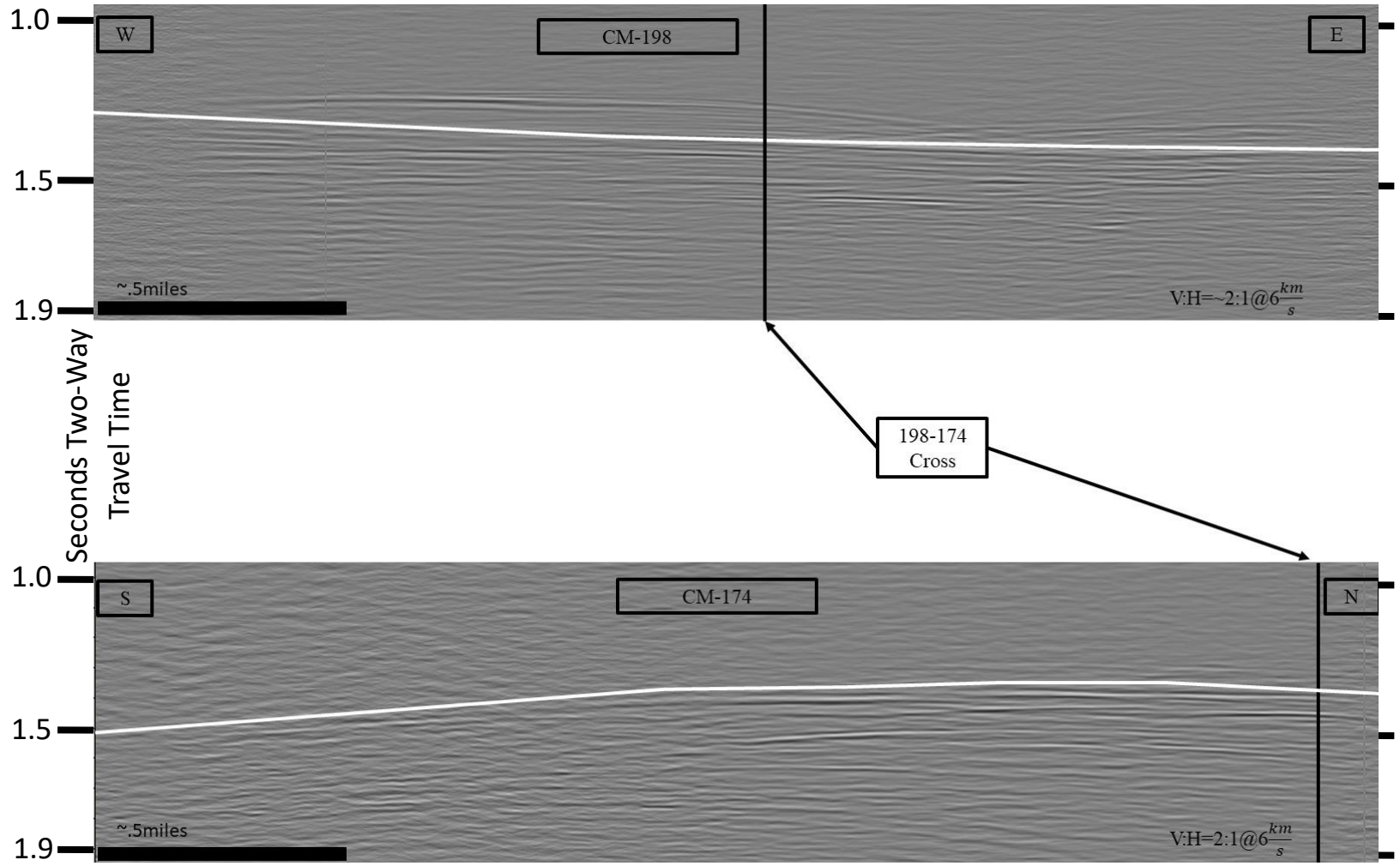

Figure 29: Interpretation of Precambrian interval as observed on crossing lines CM-198 and 174. The tops of internal Precambrian reflectors is traced in white. Black vertical lines indicate the locations on the seismic lines where the two cross.

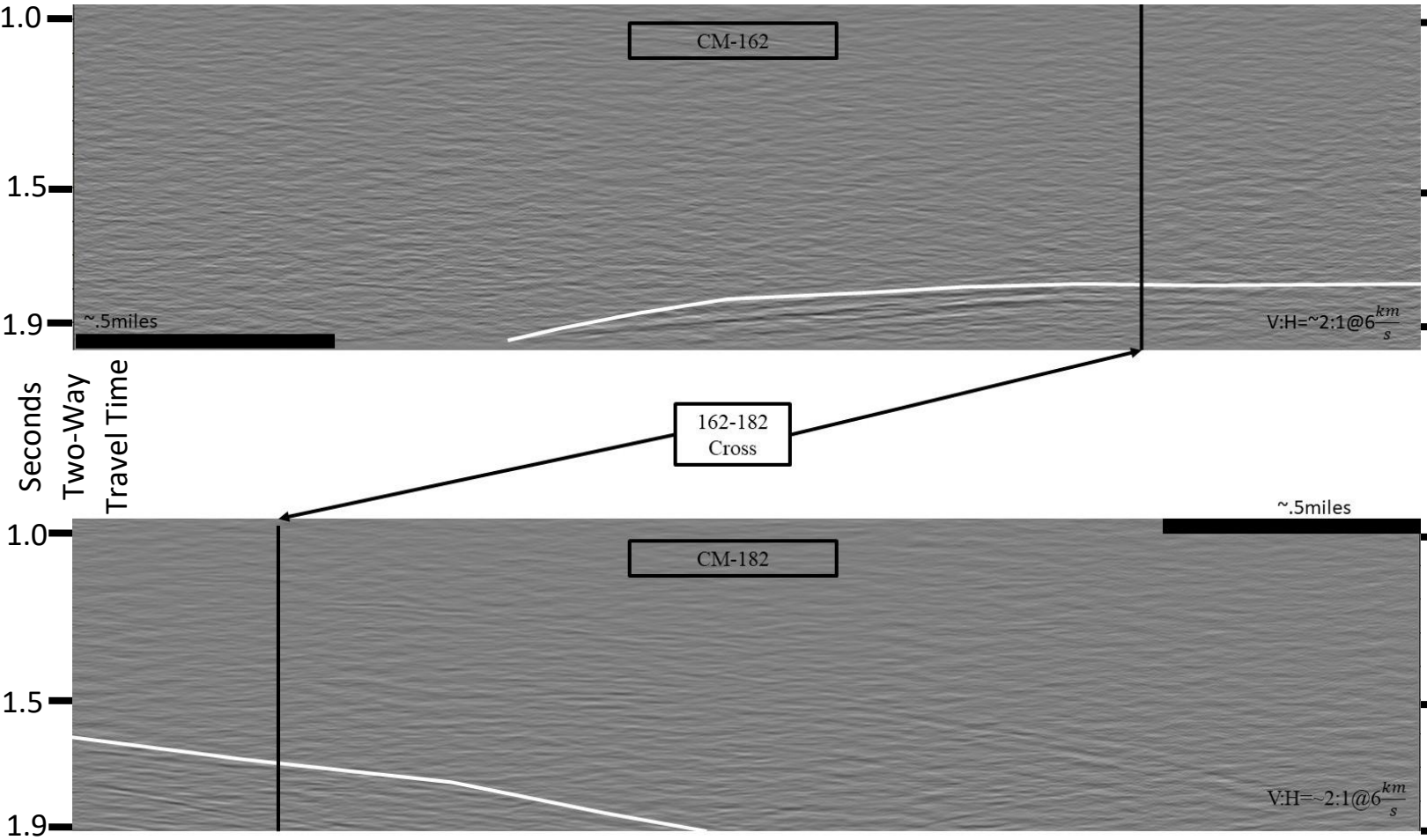

Figure 30: Crossing seismic lines CM-162 and 182 that mark the SW corner of the seismic data set examined in this study. Internal Precambrian interval reflectors are correlated between the two lines. The top of the reflectors interpreted to be indicative of real structures are traced in white. The approximate location where each line crosses the other is indicated by the vertical black line.

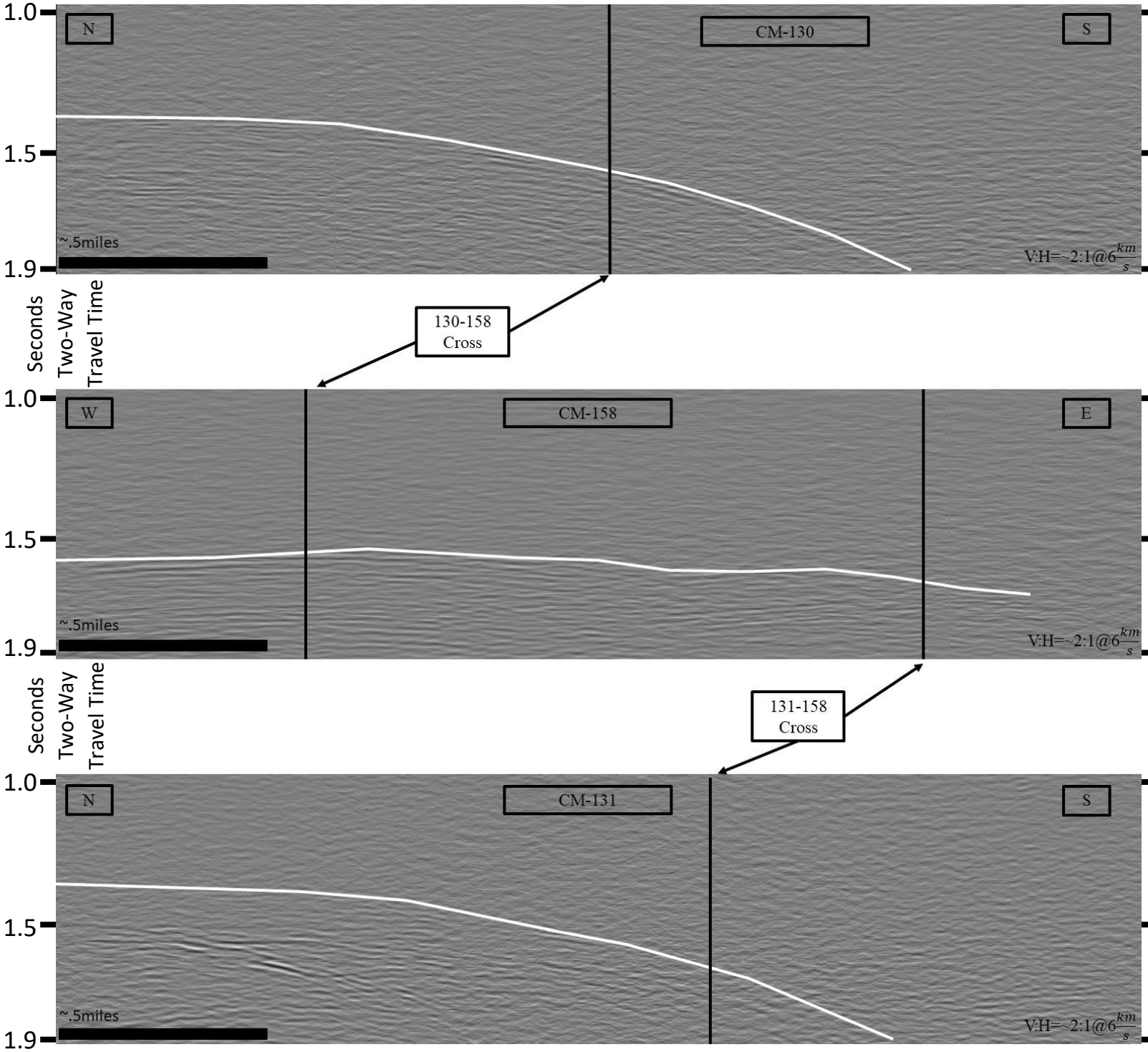

Figure 31: The Precambrian interval as interpreted on CM-130, 131 and 158. Like seismic lines CM-162 and 182, reflectors observed on CM-130 and 131 drape off the bottom edge of the section prior to reaching the end. The termination of these reflectors on the eastern most portion of CM-158 is unapparent and is as likely a product of low-fold edge affected data as it is a real termination.

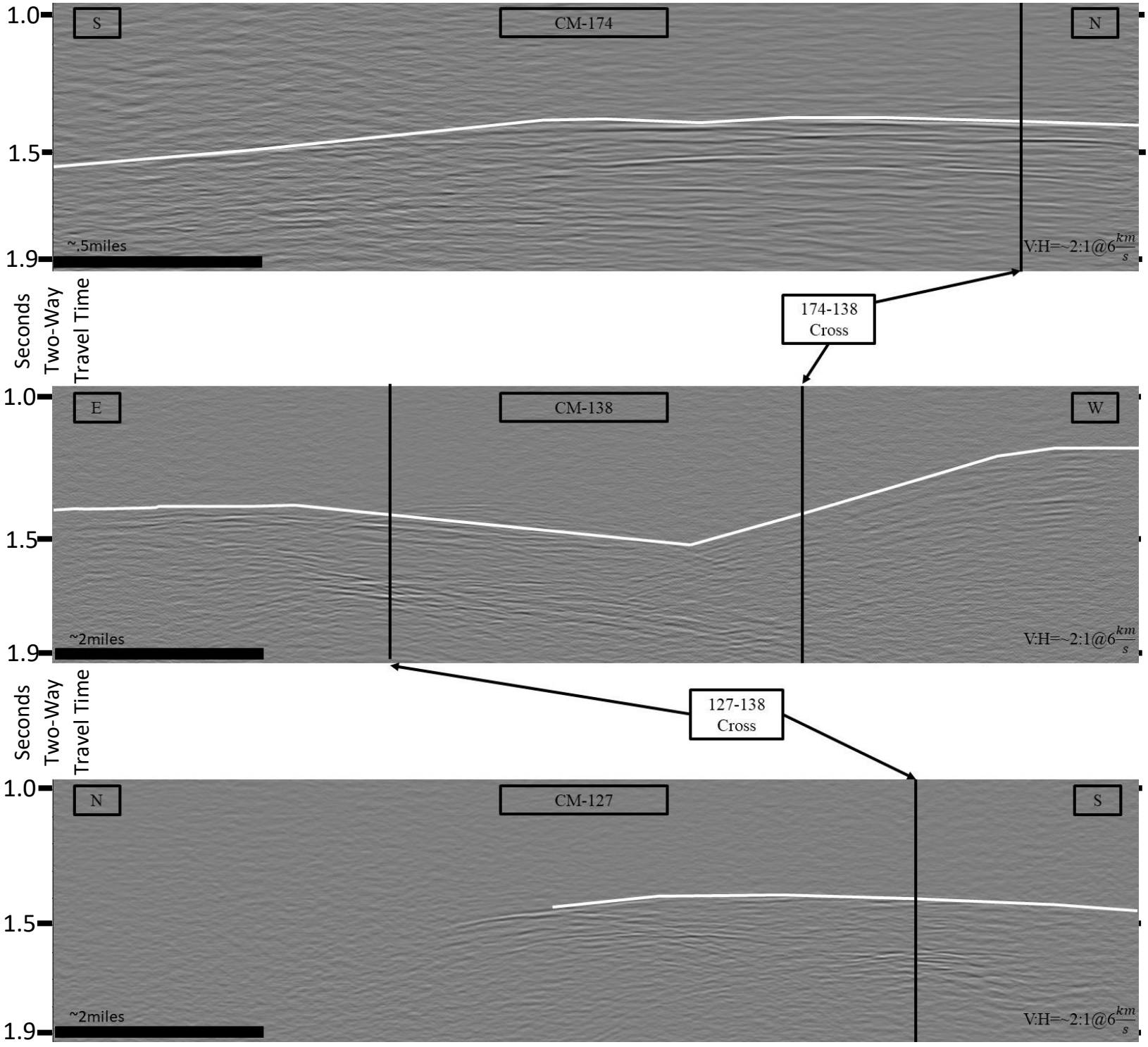

Figure 32: Precambrian interval interpretation of crossing seismic lines CM-174,138 and 127. Reflectors from this interval can generally be traced from line to line.

4.2 Gravity Data

4.2.1 Crustal Observations

Even without the application of the depth to bedrock correction, the gravity data set collected for this study is dominated by a positive gravity anomaly that is only partially captured by the data set (Fig. 33A). This anomaly trends E-W across CM-127 and is further smoothed and broadened by the correction for depth to bedrock (Fig. 33B). The positive anomaly observable on the completely reduced data set encompasses nearly all of the seismic sections within the extent of the gravity data set. The exception being at the southern end of seismic lines CM-130 and CM-131 where the reflections can be observed draping off the bottom of the section. This significant change in gravity signature could be indicative of a simple deepening of the internal Precambrian interval structures of Zone C. However, it is also likely to represent the termination or rounding off of the structure. There is no directly observable correlation between the gravity data set and the termination observed on seismic line CM-127 save the north negative slope away from the highest gravity measurements that dominate the northern portion of the western most edge of the data set. The relationship between the gravity data and seismic line CM-127 could be further evaluated through the expansion of the present gravity data set which could allow further interpretational reductions, such as removal of the regional gradient via surface fitting.

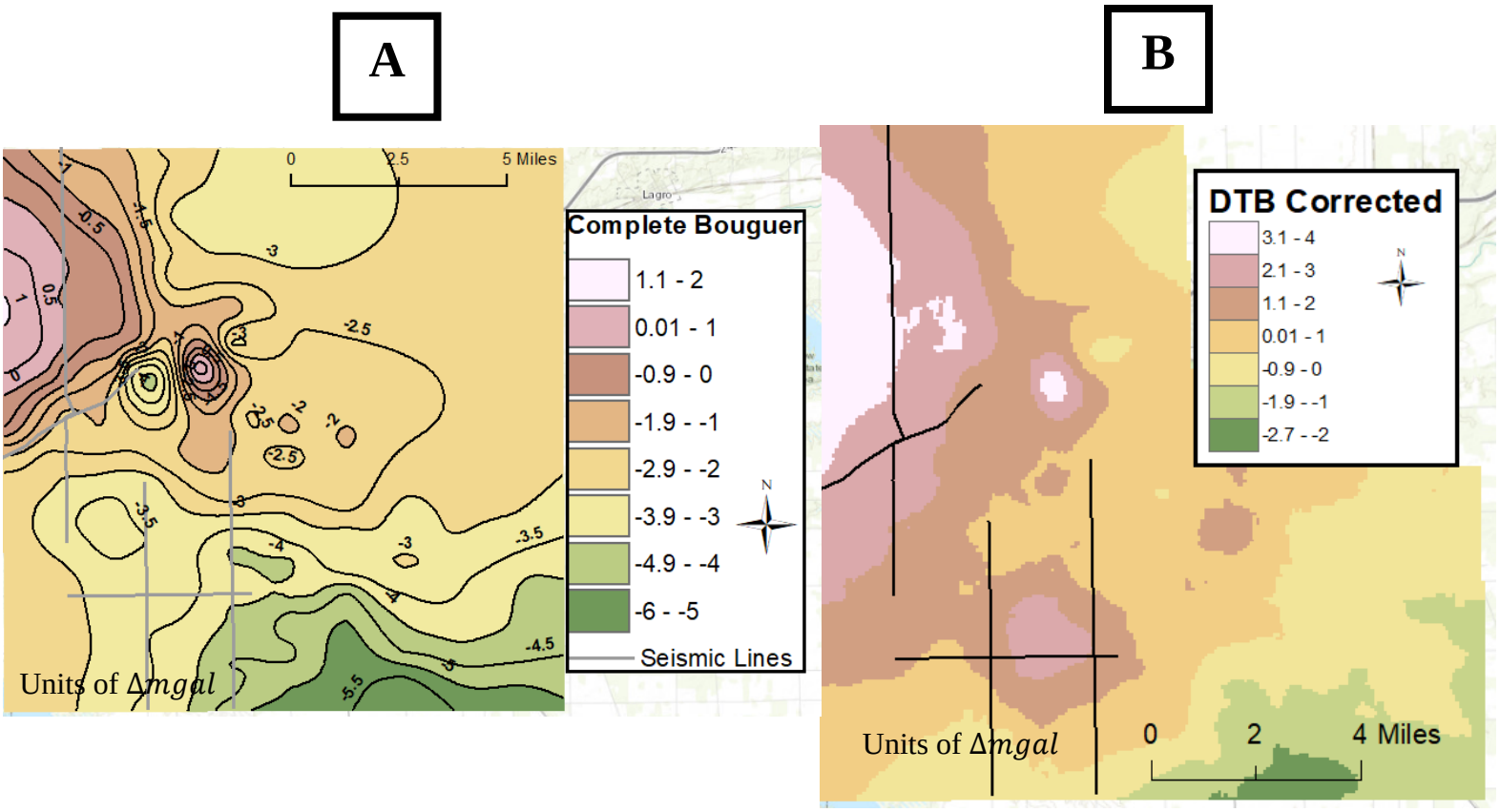

Figure 33: (A) Gravity map derived of newly acquired data reduced to the complete Bouguer anomaly. This map along with other gravity map derived of this study features units of $\Delta milligals$ which quantifies the change in the gravity field with respect to the datum station. **(B)** The depth to bedrock corrected complete Bouguer anomaly. Depth to bedrock correction proves to remove much of the near surface high frequency gravity signatures that are considered to be noise with respect to this study.

4.2.2 Near-Surface Observations

The depth to bedrock in the region dramatically varies from less than ~2 ft (~0.6 m) to 200+ ft (61+ m). Bedrock depths greater than ~200 ft (~61+ m) are interpreted to represent the primary channel of the Teays River which once flowed westward across the area. The low density glacial drift in the buried valley appears to be expressed by the bend in the gravity contours observable on the complete Bouguer anomaly map trending from the SE corner of the map to the west-central edge (Fig. 34 A and B). This observation is supported by both the Indiana DNR's unconsolidated aquifer system map as well as the bedrock elevation map produced by this study. A second notable feature occurs as a gravity low in the middle of the larger positive gravity anomaly interpreted to be indicative of internal Precambrian crystalline structure. This gravity low, though appearing at first glance to be a solitary negative anomaly, branches from the location of the Teays River Valley toward the northern portion of the gravity map (Fig. 34A). This feature, appearing to have direct correspondence to the Teays River Valley, is therefore interpreted to be a tributary bedrock valley of the Teays (Fig. 34B). This interpretation is corroborated by the pattern of bedrock topography from water well data from the Indiana DNR database as well as additional bedrock depths from the HVSR data collected in this study (Fig. 34C).

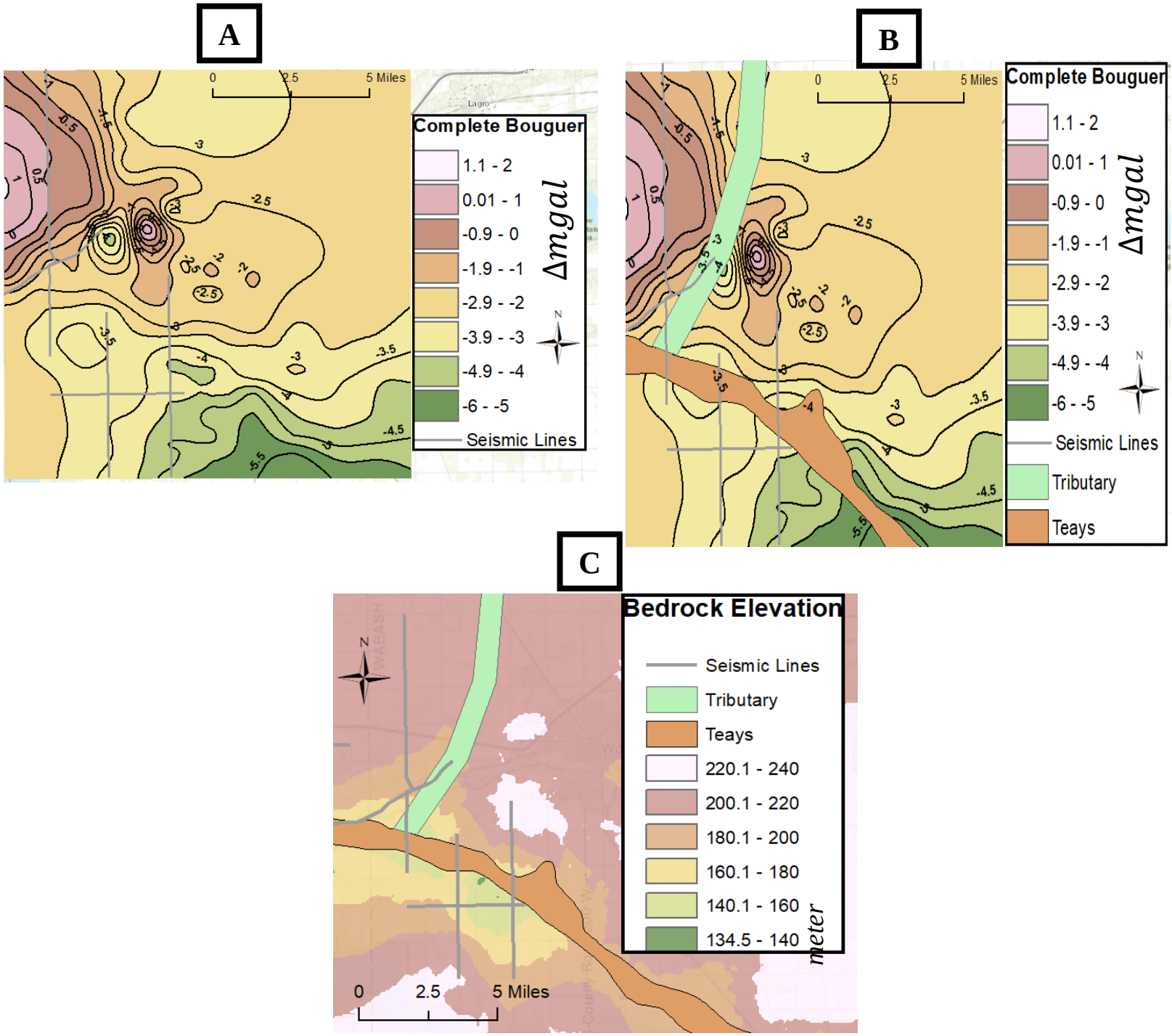

Figure 34: (A) The complete Bouguer anomaly map has two features interpreted by this study to be indicative of near surface features. The first of these features is represented by the NW trending bend in major contours beginning from the very SE portion of the map. The other cuts directly across the major positive feature in a N-S fashion and appears to be linked to the other major event. **(B)** The major event bending contours correlates very well with the Indiana DNR's placement of the ancient bedrock valley belonging to the Teays river which was originally interpreted by the Indiana DNR from water well data. The second feature cutting across the main positive feature is a new interpretation derived of this study and is interpreted to be a tributary of the Teays River. **(C)** Bedrock elevation map in units of meters. Data for this map was derived from HVSR data collected by this study and water well data collected from the Indiana DNR's water well database.

4.3 Aeromagnetic Data

4.3.1 Local Observations

The local magnetic morphology in and around the location of the ten seismic lines, as observed on the residual magnetic anomaly map (Fig. 35A), is characterized by a general magnetic high, herein referred to as the Wabash-Miami anomaly (WMA). The WMA has relatively little to no internal magnetic relief but is bordered by sharply rising gradients combined with several dipole magnetic anomalies that are relatively small in both magnitude and geographic extent. This magnetic morphology is commonly shared by granitic ring complexes across the world. Examples of such complexes include the Ossipee Mountains of eastern New Hampshire (Fig. 36), the Riruwai Younger complex of Nigeria, and the several complexes of the Svecofennian domain located in Eastern Europe (Kisvarsanyi, 1980; Olasehinde et al., 2012; Sharkov, 2010). The St. Francois Mountains of SE Missouri also feature several granitic ring complexes; however, the magnetic signature there cannot be used for comparison as the aeromagnetic data flown over that area is of insufficient quality to make such a comparison. Igneous complexes herein referred to as granitic ring complexes have also been referred to as rapkivi ring complexes, ring dykes and anorogenic granite complexes in other publications.

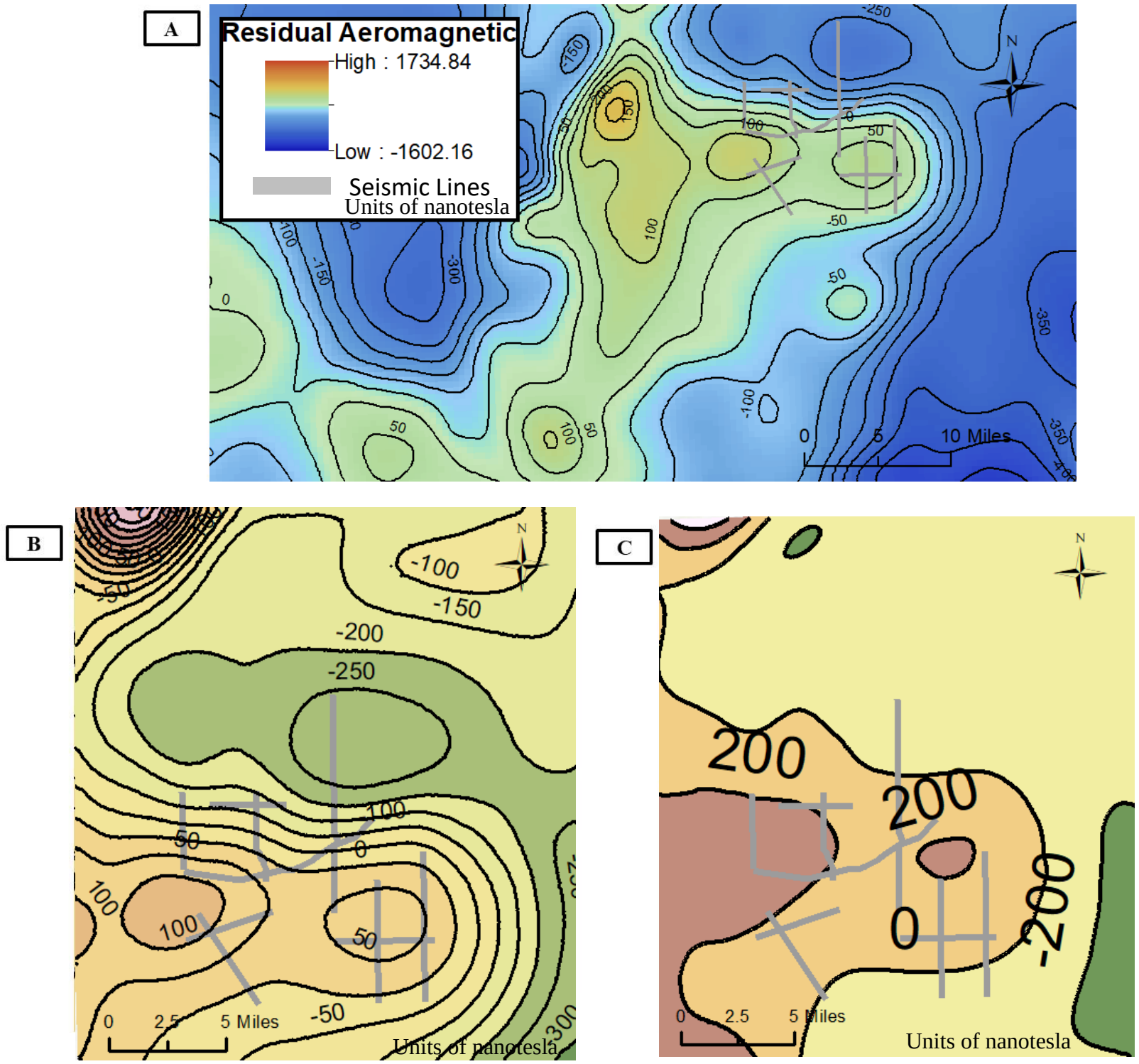

Figure 35: (A) Residual aeromagnetic map featuring units of nanotesla. This map demonstrates the general relationship between the seismic data examined by this study and the primarily positive nature of the surrounding residual magnetic field. Residual magnetic field refers to data that has been diurnally corrected and reduced from Earth's ambient magnetic as determined by the International Geomagnetic Reference Field (IGRF). **(B)** Residual aeromagnetic Map zoomed in around the area of the seismic lines which further demonstrates the sharp rise in the magnetic field at the edges of the anomaly. **(C)** Reduced to pole aeromagnetic map.

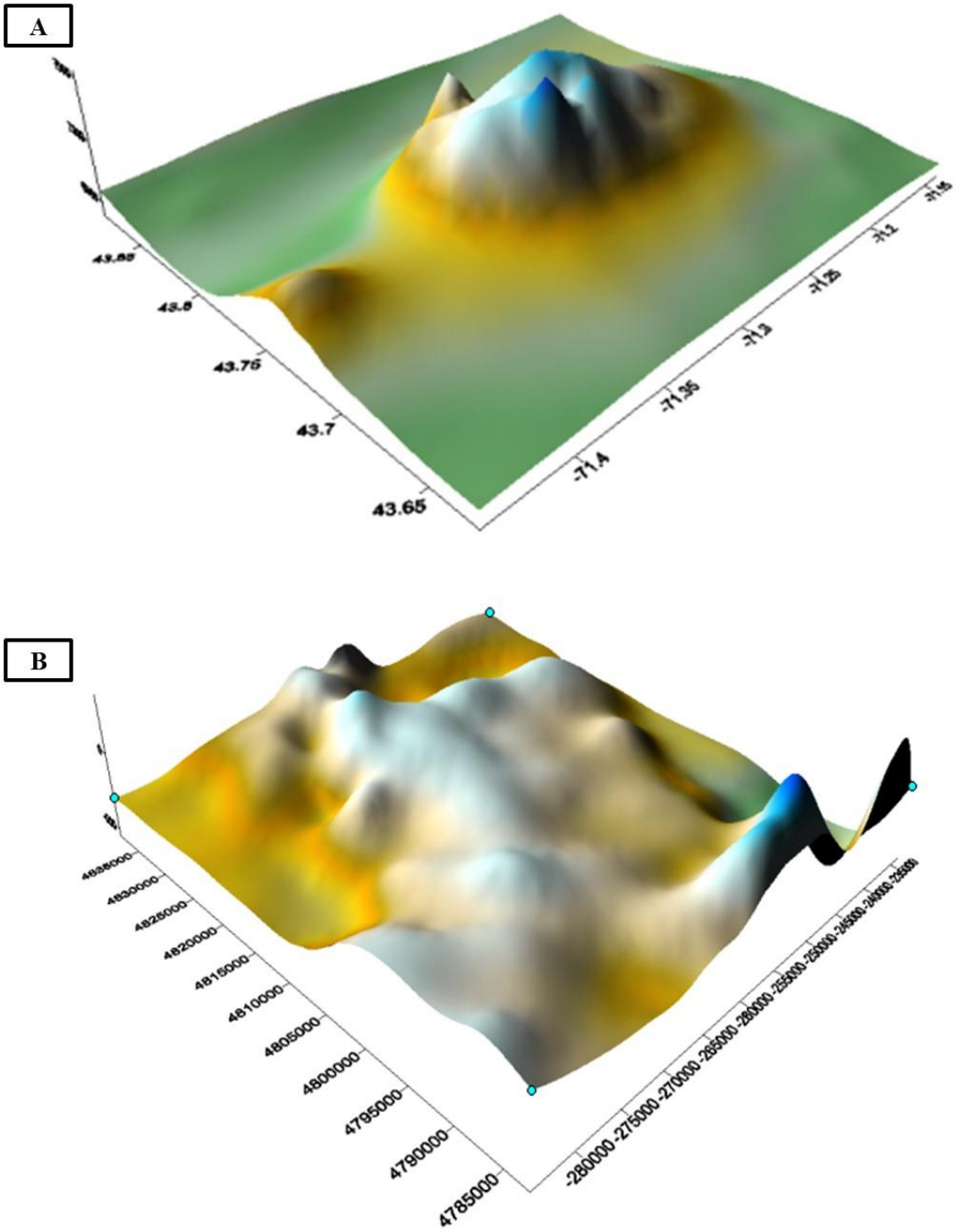

Figure 36: (A) Aeromagnetic signature of the Ossipee Mountain ring dyke complex of Carroll County, New Hampshire. This igneous feature comprises ~275 square miles and completely outcrops at the surface. **(B)** Aeromagnetic signature of the WMA. Its source is interpreted by this study to be buried at an average depth of ~2.5miles.

4.3.2 Regional Observations

The magnetic morphology of the state of Indiana can appear very diverse and complex if only local observations from small portions of the entire region are considered. However, the complexity appearing in smaller map sections begins to turn into interpretable regional patterns as larger portions of the state are observed. The magnetic morphology of the state is defined by approximately three different zones separated by a N-S trending magnetic liniment and a gradational N-S change. The N-S trending lineament splits the state into eastern and western portions. The eastern portion of the state is characterized by sharp gradients and large overlapping circular anomalies (Fig. 37). The western portion of the state is characterized by complex overlapping gradients and small sharp anomalies in the north that grade into long wavelength less complex gradients and large anomalies to the south.

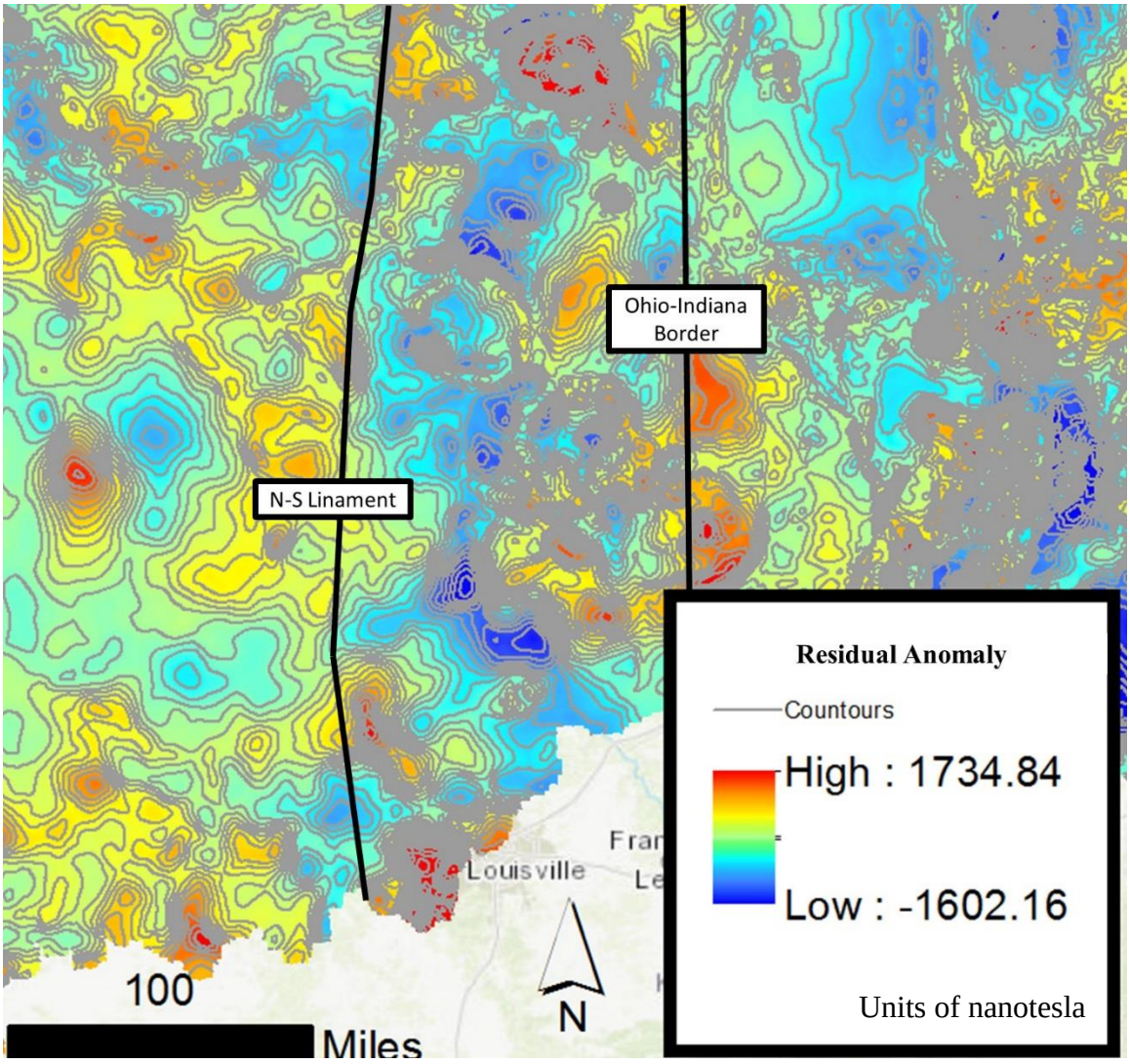

Figure 37: Major Indiana magnetic liniments that appear to separate Indiana into three different zones which feature different magnetic morphologies. The WMA fall in the eastern part of Indiana which is dominated by positive aeromagnetic ring features.

The WMA borders the major N-S liniment to the east. The east zone is dominated by ring-like magnetic structures with similar magnetic morphologies to the WMA. The largest and most apparent of these features is located to the NE of the WMA in the vicinity of Fort Wayne, Indiana (Fig. 38). This feature has been historically interpreted as a NW-SE trending rift system and is thought to be a possible southward extension of the MCR system. The interpretation of the Fort Wayne Anomaly (FWA) as being the product of a rift system is based on little evidence consisting of diffuse gravity stations, aeromagnetic data, and a single Precambrian core sample from one of the two deep boreholes drilled within the vicinity. There appears to be a general trend in the eastern ring features as they appear to become less apparent towards the south. This seems likely a result of the masking of the EGRP igneous terrain by non-magnetic Late Precambrian to Paleozoic sedimentary rocks.

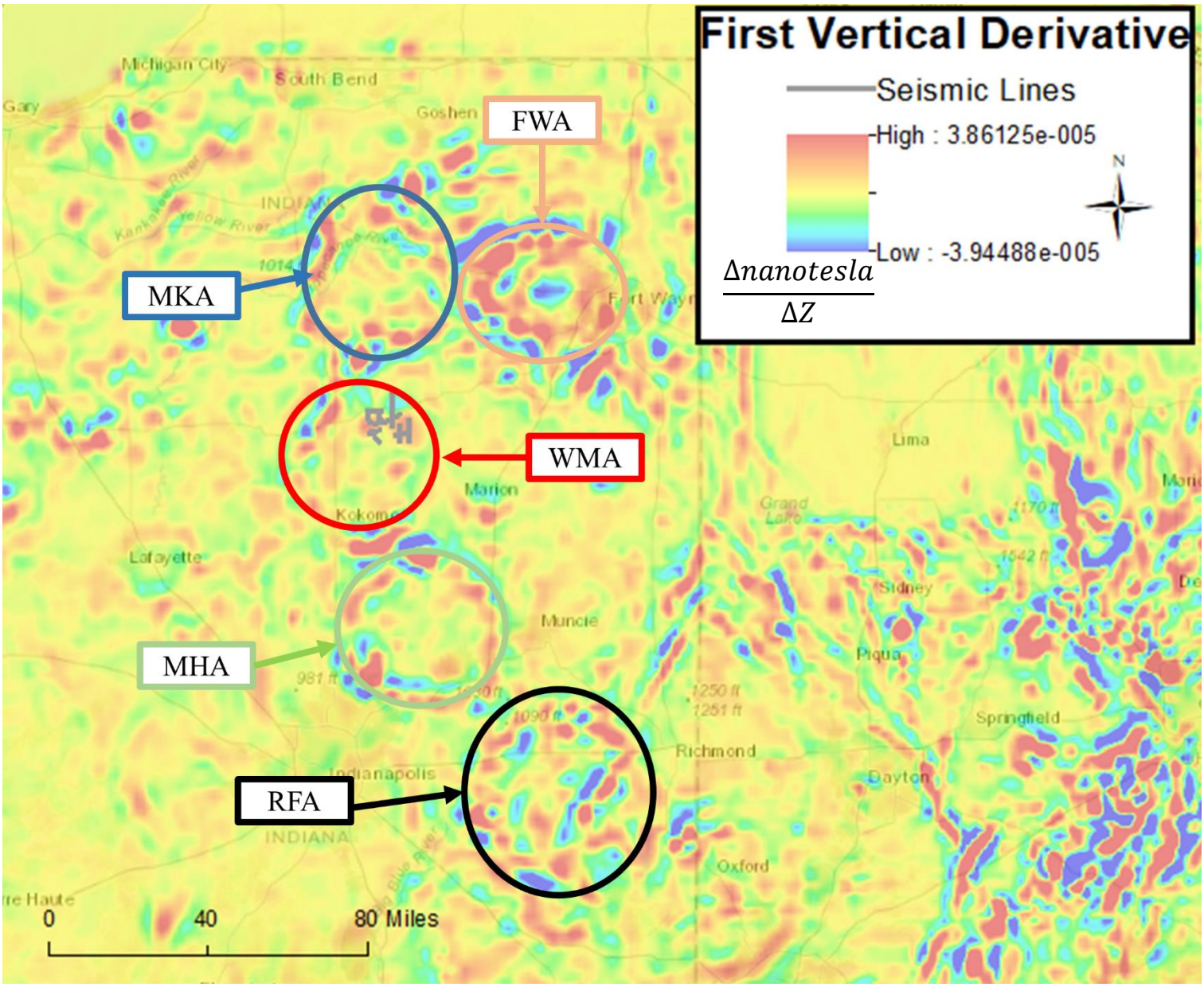

Figure 38: Identification and nomenclature propose by this study for the ring features that dominate the eastern portion of Indiana. The abbreviations can be expanded into the following designations: FWA=Fort Wayne Anomaly; MKA=Marshall-Kosciusko Anomaly; WMA: Wabash-Miami Anomaly; MHA=Miami-Howard Anomaly; RFA=Rush-Franklin Anomaly.

4.4 Geologic Implications

The ten seismic lines gathered by CountryMark are conveniently located on the northern edge of the prominent aeromagnetic ring structure that is the WMA. The only portion of a seismic line that obviously crosses the boundary of the WMA is the northern portion of CM-127. A strong correlation exists between the crossing of CM-127 and the zero zone of the first vertical derivative crudely representing the boundary of the body inducing the observed magnetic anomaly (Fig. 39). Other lines that feature extinctions of the internal Precambrian seismic interval include CM-130,131,162 and 182. The reduced to pole local aeromagnetic anomaly in Figure 35C suggests that this interval as shown on CM-130 and 131 is terminating or rounding off within the plane of these lines, but likely in a dissimilar fashion to what is observed on CM-127. This along with the interpreted character of the internal reflectors occurring within the Precambrian seismic interval on the CountryMark lines and the geometry of the positive gravity anomaly in the area suggests that the outer ring of the WMA is dominated by rocks with a greater magnetic susceptibility and higher density than both the surrounding EGRP country rock and the rock within the center of the ring structure. These observations are consistent with other interpretations of ring dyke/granite complexes observed within approximately the same time interval across the world, as well as with geophysical observations of what has been interpreted to likely be mafic sill complexes in the western portion of the EGRP (McBride et al., 2015).

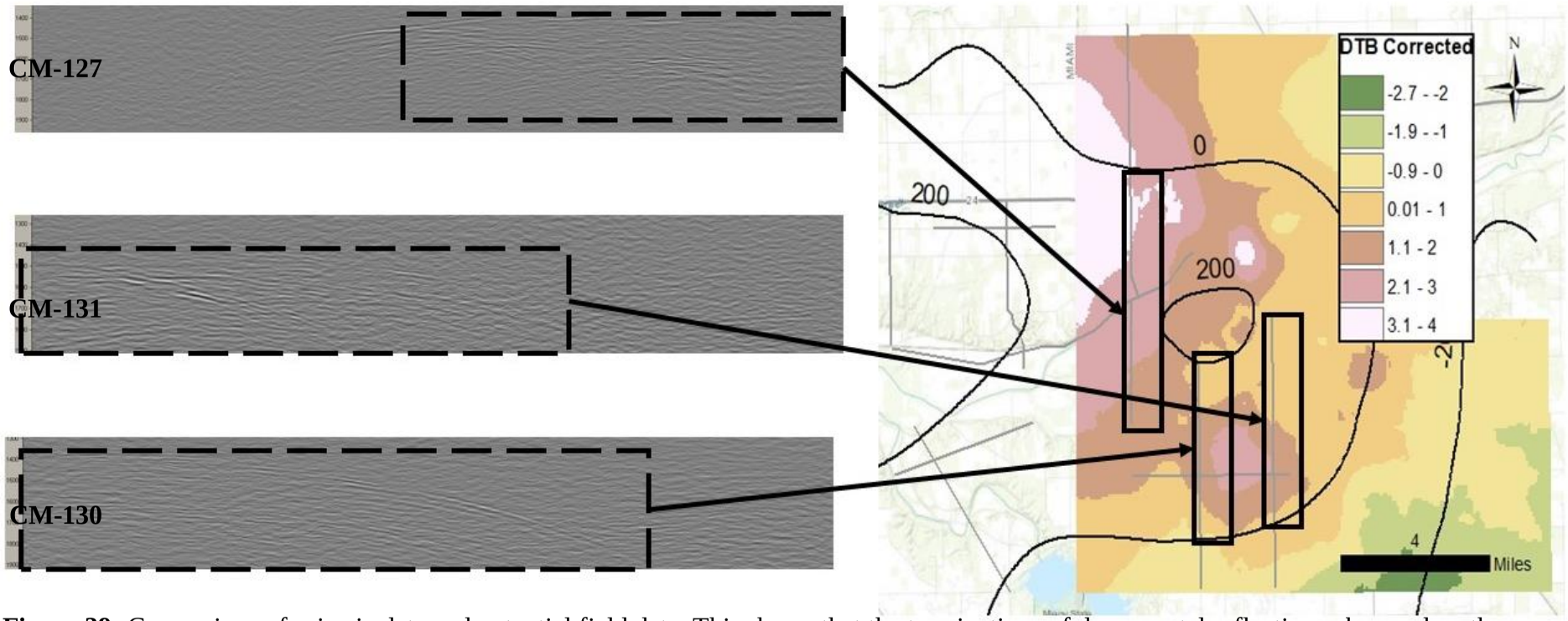

Figure 39: Comparison of seismic data and potential field data. This shows that the terminations of deep crustal reflections observed on the seismic data correlates well with the zero contour of the reduced to pole aeromagnetic data and the depth to bedrock corrected gravity. This one to one correlation confirms that deep crustal reflections are composed of rocks that are both denser and more magnetic than the overlying EGRP granites and Paleozoic strata.

If the geophysical anomaly dominating the Wabash-Miami area is a granitic ring complex, then its formation is likely analogous to those observed in the St. Francois Mountains. The leading theory for the development of granitic ring complexes observed in the St. Francois Mountains was first developed by Kisvarsnyi (1980) who championed a three-step process that began with the evacuation of a cauldron followed by caldera subsidence and collapse and concluded with a final interval of pluton resurgence and doming. If the anomalies represent a mafic sill complex then they may be derived of the mafic magmas thought to be the underplating heat source giving rise to the silicic crustal melt making up the majority of the EGRP.

The present study area is east of the Sm-Nd line of Bickford et al. (2015) which suggests that the silicic material of this part of the EGRP was derived from juvenile outboard arcs that were quickly accreted to the eastern portion of the NAMC craton before being remobilized ~1.27 Ga (Bickford et al., 2015). Whatever the geologic scenario, it is likely that the WMA anomaly and the others like it represent the final gasp of EGRP magmatism occurring around ~1.27 Ga (Bickford et al., 2015).

5.0 Conclusion

5.1 Summary

The primary goal of this study was to use ten newly available industry seismic reflection surveys to develop a reasonable description of the upper crust near Wabash, Indiana. Significant correlation between seismic anomalies within the Precambrian interval and the anomalies observed on potential field maps (Fig. 40) lead to an interpretation of the Precambrian underlying the area to be a possible mafic sill complex as part of a granitic ring complex. The development of such features represent an event of magmatism occurring in the latest stages of EGRP evolution. Though the findings of this study are consistent with observations of other EGRP geophysical evidence and Bickford et al. (2015) broad theory of EGRP evolution, the conclusions of this study simply establish a working hypothesis which could be further tested by the application of both geophysical and borehole exploration.

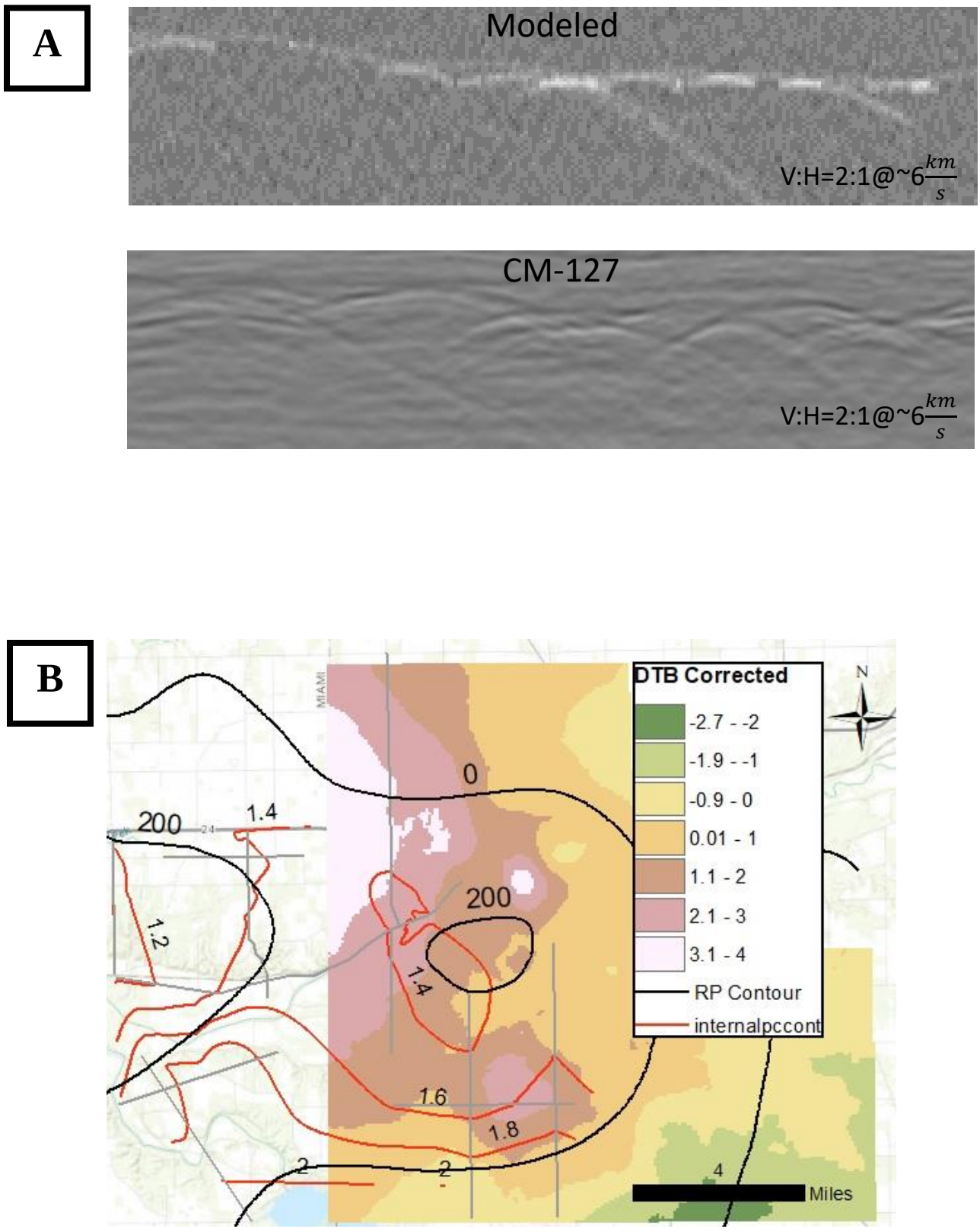

Figure 40: (A) Modeled St. Francois Mountains results compared to the actual seismic expression of the Precambrian unconformity as observed on CM-127. **(B)** DTB corrected gravity map with reduced to pole aeromagnetic contours (black) deep crustal reflection contours (red) overlain.

5.2 Remaining Questions and Future Work

The EGRP is one of the most enigmatic provinces of the North American Precambrian crust. This is primarily due to the lack of exposure and an almost 20-year, and counting, lapse of interest after a flurry of analysis of most available borehole and geophysical data. This study hopes to stimulate a revitalized interest represented by thesis projects executed by the Wright State University geophysical group. In general, how can newly available industry seismic data, and possible future academic seismic transects within the region of EGRP aeromagnetic ring anomalies shed light upon the evolution of the province.

Importantly, the spotty gravity database of the EGRP region should be improved upon, which would include an evaluation of the older data sets and a more accessible archive system for potential field data. A completion of the gravity data set could help define targets for deep 2.5D seismic reflection, wide-angle reflection, refraction transects that would serve as a basis for higher resolution 3D seismic reflection experiments.

To further address fundamental questions of EGRP evolution will also require a broader multi-institution effort that would require a significant amount of industry and academic support, but the Wright State geophysical group is already mining the newly available industry data to seek answers and also to better couch the questions.

References

Anderson, J. L., & Cullers, R. L., 1978. Geochemistry and evolution of the Wolf River batholith, a late Precambrian rapakivi massif in north Wisconsin, USA. Precambrian Research, 7(4), 287-324.

Anderson, J.L., 1983. Proterozoic anorogenic granite plutonism of North America: Geological Society of America Memoirs, v. 161, pp.133-154.

Rudman, A.J., and Blakely, R.F., 1965. A Geophysical Study of a Basement Anomaly in Indiana: GEOPHYSICS, v. 30, no. 5, p. 740-761.

Atekwana, E.A., 1996. Precambrian basement beneath the central Midcontinent United States as Interpreted from Potential Field Imagery: Geological Society of America Special Papers, v. 308, p. 33-44.

Bickford, M., Van Schmus, W., Karlstrom, K., Mueller, P., and Kamenov, G., 2015. Mesoproterozoic trans-Laurentian magmatism; a synthesis of continent-wide age distributions, new SIMS U/Pb ages, zircon saturation temperatures, and Hf and Nd isotopic compositions: Precambrian Research, v. 265, p. 286-312.

Branch of Geophysics, 1989. Potential Field Geophysics Programs for VAX 7xx Computers: USGS Open File Report 89-115A.

Cordell, L.E., Phillips, J.D. and Godson, R.H., 1992. US Geological Survey Potential-Field Geophysical Software Version 2.0: USGS Open-File Report, no. 97-725.

Corrigan, D., Pehrsson, S., Wodicka, N., & De Kemp, E., 2009. The Palaeoproterozoic Trans-Hudson Orogen: a prototype of modern accretionary processes. Geological Society, London, Special Publications, 327(1), 457-479.Cornell University, Consortium for Continental Reflection Profiling (COCORP).

Culotta, R.C., Pratt, T., and Oliver, J., 1990. A Tale of Two Structures: COCORP's Deep Seismic Surveys of the Grenville Province in the Eastern US Midcontinent: Geology, v. 18, p.646-649.

Denison, R.E., Lidiak, E.G., Bickford, M.E. and Kisvarsanyi, Eva. B., 1984. Geology and Geochronology of Precambrian Rocks in the Central Interior Region of the United States: Geological Survey Professional Paper, no. 1241-C.

Drahovzal, J.A., 1997. Proterozoic sequences and their implications for Precambrian and Cambrian geologic evolution of western Kentucky: Evidence from seismic-reflection data: Seismological Research Letters, v. 68, no. 4, p.553-56

Droste, J. B., & Shaver, R. H., 1983. Atlas of early and middle Paleozoic paleogeography of the southern Great Lakes area (No. 32). State of Indiana, Dept. of Natural Resources, Geological Survey.

Emslie, R. F., 1978. Anorthosite massifs, rapakivi granites, and late Proterozoic rifting of North America. Precambrian Research, 7(1), 61-98.

Evans, D. A., & Mitchell, R. N., 2011. Assembly and breakup of the core of Paleoproterozoic–Mesoproterozoic supercontinent Nuna. Geology, 39(5), 443-446.

Hammer, S., 1939. Terrain Corrections for Gravimeter Stations: Geophysics, v. 4, no. 3, p.184-194.

Hansen, M. C., 1995. The Teays River: Ohio Department of Natural Resources. Division of Geological Survey GeoFacts, 10(2).

Hauser, E.C., 1993. Grenville foreland thrust belt hidden beneath the eastern US midcontinent: Geology, v. 21, no. 1, pp.61-64.

Henderson, R. G., & Zietz, I. 1949. The computation of second vertical derivatives of geomagnetic fields. Geophysics, 14(4), 508-516.

Henderson, J.R. and Zietz, I., 1958. Interpretation of an Aeromagnetic Survey of Indiana: Geological Survey Professional Paper, no. 316-B.

Hildenbrand, T., 1983. FFTFIL: A filtering program based on two-dimensional Fourier analysis of geophysical data: USGS Open-File Report, no. 83-237.

Hill, P., Kucks, R., and Ravat, D., 2009. Aeromagnetic and Aeroradiometric Data for the Conterminous United States and Alaska from the National Uranium Resource Evaluation (NURE) Program of the U.S. Department of Energy: USGS Open Report, no. 2009-1129.

Hinze, W.J., Von Frese, R.R.B., and Saad, A.H., 2013. Gravity and Magnetic Exploration: Principles, Practices and Applications: Cambridge.

Hoffman, P.F., 1988. United Plates of America, The Birth of a Craton: Early Proterozoic Assembly and Growth of Laurentia: Annual Review Of Earth And Planetary Sciences, v. 16, no. 1, p. 543.

Indiana Department of Natural Recourses, 2018, Water Well Database.

Indiana Geological Survey, 2015, Petroleum Database Management System, Well Records.

Indiana Geological Survey, 2017, Core Library.

Indiana Spatial Data Portal. The Trustees of Indiana University, 2012, 2017.

Karlstrom, K. E., Bowring, S. A., & Conway, C. M. 1987. Tectonic significance of an Early Proterozoic two-province boundary in central Arizona. Geological Society of America Bulletin, 99(4), 529-538.

Lane, J.W. Jr., White, E. A., Steele, G.V., and Cannia, J. C., 2008. Estimation of Bedrock Depth Using the Hortizontal to Vertical (H/V) Ambient-Noise Seismic Method: Symposium on the Application of Geophysics to Engineering and Environmental Problems, p. 13.

Leetaru, H.E., and Freiburg, J.T., 2014. Litho-facies and reservoir characterization of the Mt Simon Sandstone at the Illinois Basin–Decatur Project: Greenhouse Gases Science and Technology, v. 4, p. 580–595.

Litak, R. K., & Hauser, E. C. (1992). The Bagdad reflection sequence as tabular mafic intrusions: Evidence from seismic modeling of mapped exposures. Geological Society of America Bulletin, 104(10), 1315-1325.

Magnani, M.B., Miller, K.C., Levander, A. and Karlstrom, K., 2004. The Yavapai-Mazatzal boundary: A long-lived tectonic element in the lithosphere of southwestern North America: Geological Society of America Bulletin, v. 116, no.9-10, p.1137-1142.

McBride, J.H., Leetaru, H.E., Keach, R.W. and McBride, E.I., 2016. Fine-scale structure of the Precambrian beneath the Illinois Basin: Geosphere, v. 12 no. 2, p.585-606.

Moecher, D.P., Bowersox, J.R., and Hickman, J.B., 2018. Zircon U-Pb Geochronology of Two Basement Cores (Kentucky, USA): Implications for Late Mesoproterozoic Sedimentation and Tectonics in the Eastern Midcontinenet: The Journal of Geology, v. 121, p. 25-39.

The University of Texas at El Paso, PACES, 2013. Online Gravity and Magnetic Database.

Parent, A.M., 2017. Pre-Mt. Simon Seismic Sequences below West-Central Indiana: Local Interpretation and Regional Significance: M.S. Thesis, Wright State University, Dayton, OH.

Peterman, D.J., 2016. Seismic Reflection Profiling near Middletown, Ohio and Interpretation of Precambrian Deformational Settings: M.S. Thesis, Wright State University, Dayton, OH.

Phillips, J., 1997. Potential-Field Geophysical Software for the PC, version 2.2: USGS Open-File Report, no. 97-725.

Pratt, T.L., Hauser, E.C., and Nelson, K.D., 1992. Widespread buried Precambrian layered sequences in the U.S. Mid-continent: Evidence for large Proterozoic depositional basins: American Association of Petroleum Geologists Bulletin, v. 76, p. 1384–1401.

Reynolds, J. M., 2011. An introduction to applied and environmental geophysics. John Wiley & Sons.

Rudman, A.J., Blakely, R.F., 1965. A Geophysical Study of a Basement Anomaly in Indiana: Geophysics, v. xxx, no. 5, p.740-761.

Rudman, A.J., Mead, J., Whaley, J.F. and Blakely, R.F., 1971. Geophysical analysis in central Indiana using potential field continuation: Geophysics, v. 36, no. 5, p.878-890.

Rudman, A. J., & Rupp, J. A., 1993. Geophysical properties of the basement rocks of Indiana (Vol. 55). Indiana Geological Survey.

Schulz, K., & Cannon, W. 2007. The Penokean orogeny in the Lake Superior region: Precambrian Research, v. 157, no. 1-4, p. 4-25.

Shaver, R. H., Ault, C. H., Burger, A. M., Carr, D. D., Droste, J. B., Eggert, D. L., ... & Horowitz, A. S., 1986. Compendium of rock-unit stratigraphy in Indiana—a revision: Indiana Geological Survey. Bulletin, 59, 203.

Shrake, D.L., Carlton, A.W., Wickstrom, L.H., Potter, P.E., Richard, B.H., Wolfe, P.J., and Sitler,G.W., 1991. Pre-Mount Simon Basin under the Cincinnati Arch: Geology, v. 19, p. 139–142.

Shrake, D.L., 1991. The Middle Run Formation: A Subsurface Stratigraphic Unit in Southwestern Ohio: The Ohio Journal of Science. v91, n1 (March, 1991), 49-55.

Sides, J.R., Bickford, M.E., Shuster, R.D. and Nusbaum, R.L., 1981. Calderas in the Precambrian terrane of the St. Francois Mountains, southeastern Missouri: Journal of Geophysical Research: Solid Earth, v. 86, no. B11, p.10349-10364.

Smith, V., & Leetaru, H. (2014). 2D Seismic Reflection Data across Central Illinois. University of Illinois.

Stauffer, M.R. 1984. Manikewan: An early proterozoic ocean in central Canada, its igneous history and orogenic closure: Precambrian Research, v. 25, p. 257-281.

Telford, W.M., Geldart, L.P., Sheriff, R.E., 1990. Applied Geophysics: Cambridge University Press.

Van Schmus, W.R., Bickford, M.E. and Turek, A., 1996. Proterozoic geology of the east-central Midcontinent basement: Geological Society of America Special Papers, v. 308, p.7-32.

Van Schmus, W.R., Bickford, M.E., Sims, P.K., Anderson, R.R., Shearer, C.K., and Treves,S.B., 1993b. Proterozoic geology of the western midcontinent basement: Geological Society of America Conference Paper, Boulder, CO., Geology of North America, v. C-2, p. 239–259.

Webring, M., 1981. MINC: A gridding program based on minimum curvature. USGS Open-File Report, no. 81-1224.

Welder, J., 2014. Seismic Interpretation and Well Log Analysis of Jay County, Indiana, Focused on Lithologic Units below the Mt. Simon Formation: M.S. Thesis, Wright State University, Dayton, OH.